Biochimica et Biophysica Acta 1840 (2014) 3320–3334

Contents lists available at ScienceDirect

Biochimica et Biophysica Acta

journal homepage: www.elsevier.com/locate/bbagen

Methyl pyruvate rescues mitochondrial damage caused by *SIGMAR1* mutation related to amyotrophic lateral sclerosis

Hideaki Tagashira [1], Yasuharu Shinoda [1], Norifumi Shioda, Kohji Fukunaga *

Department of Pharmacology, Graduate School of Pharmaceutical Sciences, Tohoku University, Aoba-ku, Sendai, Japan

A R T I C L E   I N F O

Article history:
Received 18 February 2014
Received in revised form 4 August 2014
Accepted 20 August 2014
Available online 29 August 2014

Keywords:
Sigma-1 receptor
Endoplasmic reticulum stress
Autophagy
Neurodegeneration
Amyotrophic lateral sclerosis

A B S T R A C T

Background: Amyotrophic lateral sclerosis (ALS) is a disease caused by motor neuron degeneration. Recently, a novel *SIGMAR1* gene variant (p.E102Q) was discovered in some familial ALS patients.
Methods: We address mechanisms underlying neurodegeneration caused by the mutation using Neuro2A cells overexpressing σ_1R^{E102Q}, a protein of a *SIGMAR1* gene variant (p.E102Q) and evaluate potential amelioration by ATP production *via* methyl pyruvate (MP) treatment.
Results: σ_1R^{E102Q} overexpression promoted dissociation of the protein from the endoplasmic reticulum (ER) membrane and cytoplasmic aggregation, which in turn impaired mitochondrial ATP production and proteasome activity. Under ER stress conditions, overexpression of wild-type σ_1R suppressed ER stress-induced mitochondrial injury, whereas σ_1R^{E102Q} overexpression aggravated mitochondrial damage and induced autophagic cell death. Moreover, σ_1R^{E102Q}-overexpressing cells showed aberrant extra-nuclear localization of the TAR DNA-binding protein (TDP-43), a condition exacerbated by ER stress. Treatment of cells with the mitochondrial Ca^{2+} transporter inhibitor Ru360 mimicked the effects of σ_1R^{E102Q} overexpression, indicating that aberrant σ_1R-mediated mitochondrial Ca^{2+} transport likely underlies TDP-43 extra-nuclear localization, segregation in inclusion bodies, and ubiquitination. Finally, enhanced ATP production promoted by methyl pyruvate (MP) treatment rescued proteasome impairment and TDP-43 extra-nuclear localization caused by σ_1R^{E102Q} overexpression.
Conclusions: Our observations suggest that neurodegeneration seen in some forms of ALS are due in part to aberrant mitochondrial ATP production and proteasome activity as well as TDP-43 mislocalization resulting from the *SIGMAR1* mutation.
General significance: ATP supplementation by MP represents a potential therapeutic strategy to treat ALS caused by *SIGMAR1* mutation.

1. Introduction

Amyotrophic lateral sclerosis (ALS, OMIM #105400) is a disease caused by motor neuron degeneration. ALS patients exhibit diverse pathologies such as endoplasmic reticulum (ER) stress and mitochondrial dysfunction [1,2]. Five to ten percent of ALS patients have familial ALS, a form of the disease caused by genetic mutations, while the sporadic form of the disease occurs in 90–95% of patients [3]. Familial ALS-associated gene variants identified since 1993 include *superoxide dismutase 1* (*SOD1*), *vesicle-associated membrane protein-associated protein B and C* (*VAPB*, *ALS8*), *TAR DNA-binding protein* (*TARDBP*), *FUS RNA-binding protein* (*FUS*) and *chromosome 9 open reading frame 72* (*C9ORF72*) [4,5]. Several reports also document the significance of mitochondrial dysfunction, pathogenic protein aggregation and defects in the ubiquitin–proteasome system (UPS) in ALS pathogenesis [6–8]. Notably, a significant population of patients with ALS (~95%) or frontotemporal lobar degeneration (FTLD, OMIM #600274) (~45%) has TDP-43 positive inclusions in the central nervous system [9,10]. FTLD is a leading cause of dementia with or without motor neuron degeneration. ALS and FTLD are part of the same pathological spectrum [4,10]. For example, *C9ORF72* dysfunction is associated with these diseases: specifically, a hexanucleotide repeat expansion in *C9ORF72* is associated with familial ALS, sporadic ALS and familial FTLD [5].

Luty et al. reported mutations in the 3′ untranslated region (UTR) of *Sigma receptor 1* (*SIGMAR1*), which encodes the sigma-1 receptor (σ_1R), in Australian and Polish FTLD cohorts [11]. These variants (c.672*51G>T, c.672*26C>T and c.672*47G>A) were associated with dysregulated

Abbreviations: ALS, amyotrophic lateral sclerosis; DMEM, Dulbecco's minimal essential medium; ER, endoplasmic reticulum; FBS, fetal bovine serum; FTLD, frontotemporal lobar degeneration; GRP75, 75 kDa glucose-regulated protein; IP_3, inositol 1,4,5-trisphosphate; IP_3R, inositol 1,4,5-trisphosphate receptor; MAM, mitochondria-associated ER membrane; Mfn2, Mitofusin-2; PBS, phosphate-buffered saline; PERK, RNA-dependent protein kinase-like ER kinase; σ_1R, sigma-1 receptor; TMs, transmembrane domains; VDAC, voltage-dependent anion channel; ATP, adenosine triphosphate; TCA cycle, tricarboxylic acid cycle

* Corresponding author at: Department of Pharmacology, Graduate School of Pharmaceutical Sciences, Tohoku University, Aramaki-Aoba, Aoba-ku, Sendai 980-8578, Japan. Tel.: +81 22 795 6837; fax: +81 22 795 6835.
E-mail address: kfukunaga@m.tohoku.ac.jp (K. Fukunaga).

[1] These authors contributed equally to this paper.

http://dx.doi.org/10.1016/j.bbagen.2014.08.012
0304-4165/

SIGMAR1 transcription. Meanwhile, Belzil et al. reported a different *SIGMAR1* variant (c.672*43G>T) in Caucasian ALS patients who showed cognitive deficits [12]. In addition, a missense *SIGMAR1* mutation (c.304G>C), which results in substitution of glutamine for glutamic acid at amino acid residue 102 (p.E102Q), was reported in familial ALS patients [13]. Al-Saif et al. reported that overexpression of σ_1R^{E102Q} in NSC34 cells, a motor neuron-like cell line, enhanced vulnerability to ER stress and reduced cell viability [13]. Prause et al. also reported abnormal distribution of endogenous σ_1R in fibroblasts of *ALS8* patients (OMIM #608627) [14]. Although these observations suggest that mutation or mislocalization of σ_1R functions in ALS and FTLD pathologies, it is not known whether perturbations of σ_1R protein compromise motor neuron survival, and if so, what the underlying mechanism is.

σ_1R was discovered in 1976 and subsequently defined as a nonopioid receptor subtype [15,16]. Recently, Hayashi and Su reported that σ_1R preferentially localizes to the mitochondria-associated ER membrane (MAM) and functions in Ca^{2+} transport from the ER to mitochondria *via* interaction with the inositol 1,4,5-trisphosphate receptor (IP_3R) [17]. They also showed that σ_1R knockdown enhances ER stress-induced cell death [17]. Similarly, we have reported that σ_1R knockdown in neuroblastoma Neuro2A cells impairs Ca^{2+} transport through the IP_3R [18]. Conversely, we found that σ_1R overexpression enhanced mitochondrial Ca^{2+} uptake and ATP production, which improved cell survival under ER stress conditions [18]. Others have evaluated σ_1R function *in vivo* and reported that σ_1R knockout (KO) mice display motor neuron deficiency [19].

Here, we asked whether the σ_1R^{E102Q} mutation induces mitochondrial dysfunction and, if so, how that activity might induce neuronal cell death. We report for the first time that σ_1R^{E102Q} overexpression in Neuro2A cells mediates σ_1R^{E102Q} dissociation from IP_3R, which in turn impairs mitochondrial Ca^{2+} transport, ATP production and proteasome activity. More importantly, ATP depletion promoted by σ_1R^{E102Q} caused extra-nuclear localization of TDP-43 and enhanced its ubiquitination only under ER stress conditions. Finally, we discovered that pathogenic activities caused by σ_1R^{E102Q} could be rescued by ATP supplementation through treatment with methyl pyruvate (MP), a substrate in the mitochondrial tricarboxylic acid (TCA) cycle.

2. Materials and methods

2.1. Materials

Reagents and antibodies were obtained from the following sources: anti-σ_1 receptor antibody — a kind gift of Dr. Teruo Hayashi, National Institute on Drug Abuse at the National Institutes of Health, Bethesda, MD; anti-IP_3R3 — BD Biosciences, San Diego, CA; anti-LC3 antibody — MBL, Nagoya, Japan; anti-TDP-43 antibody — Sigma, St. Louis, MO; anti-ATF6 — Thermo Scientific, Runcorn, UK; anti-phospho-IRE1 — Millipore, Billerica, MA; anti-total-IRE1 — Cell Signaling Technology, Beverly, MA; anti-GRP75 — Cell Signaling Technology, Beverly, MA; anti-mitofusin 2 — Sigma, St. Louis, MO; anti-mitofusin 1 — Abcam, Cambridge, UK; anti-voltage-dependent anion channel (VDAC) — Cell Signaling Technology, Beverly, MA; anti-phospho- and total-PERK — Cell Signaling Technology, Beverly, MA; anti-GM130 — BD Biosciences, San Diego, CA; anti-19S proteasome antibody — Abcam, Cambridge, UK; anti-DsRed antibody — Clontech, Mountain View, CA; anti-SERCA — Sigma, St. Louis, MO; anti-cytochrome *c* — BD Biosciences, San Diego, CA; and anti-β-tubulin antibody — Sigma, St. Louis, MO. Methyl pyruvate (MP) and 3-methyladenine (3-MA) were purchased from Sigma-Aldrich (St. Louis, MO). Other reagents were of the highest quality available (Wako Pure Chemicals, Osaka, Japan).

2.2. Cell culture and transfection

Neuro2A cells derived from a mouse neuroblastoma C1300 tumor were obtained from the Human Science Research Resources Bank (IFO50081) (Osaka, Japan). Cells were grown in Dulbecco's minimal essential medium (DMEM) supplemented with 10% heat-inactivated fetal bovine serum (FBS) and penicillin/streptomycin (100 units/100 μg/ml) in a 5% CO_2 incubator at 37 °C. Cells were transfected with expression vectors using Lipofectamine 2000 (Invitrogen, Carlsbad, CA) [20], and analysis was performed 48 h later, as described [18,21].

2.3. Construction of expression vectors encoding mutant forms of σ_1R

Total RNAs were prepared from mouse brain hippocampus using a TRIzol LS reagent (Invitrogen, Carlsbad, CA) according to the manufacturer's protocol. mRNA was reverse-transcribed into single-stranded cDNA using an oligo(dT) primer (Promega, Madison, WI) and Moloney murine leukemia virus-reverse transcriptase (Invitrogen). σ_1R DNA sequences amplified by PCR using specific 5′- and 3′-primers were described previously [18]. DNA sequencing was provided by the Fasmac DNA Sequence Service (FASMAC Co., Ltd., Kanagawa, Japan). To construct expression vectors, PCR-amplified products were digested with XhoI and BamHI and ligated to purified XhoI- and BamHI-digested pmCherry-N1 or pEGFP-N1 vector (Clontech, Mountain View, CA) in the sense orientation. σ_1R sequences were mutated using a KOD mutagenesis kit (Toyobo, Osaka, Japan) and the following primers; F: 5′-GCAGCACATACTGGGACAGCGAGGCG-3′ R: 5′-CGCCTCGCTGTCCCAGTATGTGCTGC-3′.

2.4. Immunocytochemistry

Cultured Neuro2A cells were plated on collagen-coated glass slides at a density of $1–2 \times 10^6$ cells per 12 mm diameter coverslip. After incubation for 96 h, non-transfected or transfected cultured cells were washed 3 times in phosphate-buffered saline (PBS; pH 7.4) and fixed with 4% formaldehyde. For mitochondrial staining, Neuro2A cells were stained for 20 min with 0.02 μM MitoTracker Red CMXRos (Molecular Probes, Eugene, OR), an indicator of mitochondrial membrane potential [22], before fixation with 4% formaldehyde. After permeabilization with 0.1% Triton X-100 in PBS, fixed cells were incubated with 1% bovine serum albumin in PBS for 30 min. For immunocytochemistry, Neuro2A cells were incubated for 24 h at 4 °C with anti-cytochrome *c* antibody (1:500), anti-LC3 antibody (1:500), anti-19S proteasome antibody (1:1000), anti-GM130 antibody (1:500), anti-SERCA antibody (1:500) or anti-TDP-43 antibody (1:500) in PBS containing 1% BSA. After washing, cells were incubated for 24 h with a species-specific Alexa 594 or 488 secondary antibody in PBS containing 1% BSA. For nuclear staining, sections were incubated with DAPI (Vector Laboratories, Burlingame, CA). Immunofluorescent images were obtained with a confocal laser scanning microscope (TCS SP, Leica Microsystems, Wetzlar, Germany). Quantitation of TDP-43 distribution was performed using 5 dishes for each condition.

2.5. Immunoprecipitation and Western blot analysis

Immunoprecipitation and Western blotting were performed using previously described methods [18,23]. Immunoprecipitation analysis of σ_1R and IP_3R3 was undertaken using lysates of Neuro2A cells with or without transfection with σ_1R-mCherry or σ_1R^{E102Q}-mCherry. After immunoprecipitation with an anti-IP_3R3 antibody, immunoprecipitants were separated on SDS-PAGE and subjected to Western blot analysis using an anti-DsRed antibody. In immunoblotting analyses to determine protein levels, cultured Neuro2a cells were washed with PBS at 4 °C and stored at −80 °C until analyses were performed [23]. For assays, frozen Neuro2A cells were homogenized using methods previously described [18]. An equal amount of protein for each sample was loaded onto 7.5–15% SDS-polyacrylamide gels and transferred onto polyvinylidene difluoride membranes (Millipore Corporation, Billerica, MA). Membranes were blocked for 1 h in 5% non-fat dried milk in Tris-buffered saline plus 0.1% Tween-20 (TBS-T) and incubated with primary antibodies overnight at 4 °C. Membranes were then washed in TBS-T, incubated for 1 h with secondary antibodies, and washed in TBS-T, and blots were developed using the ECL immunoblotting detection system (Amersham Biosciences, Buckinghamshire, UK). The light-emitting signal was captured by a Luminescent Image Analyzer (LAS-4000 mini, Fuji Film, Tokyo, Japan) attached to a CCD camera. The densitometry of Western blot signals was performed using Image Gauge Ver3.0 (Science Lab, Fuji Film, Tokyo, Japan). Relative intensities of Western blot signals were expressed as a percentage of control cell band values.

2.6. Mitochondrial Ca^{2+} measurement using ratiometric-pericam-mt

Neuro2A cells were cultured on 0.01% poly-L-lysine (Sigma, St. Louis, MO)-coated glass-bottom dishes and maintained in growth medium. Transfections were performed with Ratiometric pericam targeted to the mitochondrial matrix (Ratiometric-pericam-mt/pcDNA3), a kind gift of Dr. Atsushi Miyawaki of the RIKEN Brain Science Institute (Wako City, Japan), as described in [18,24]. Briefly, 1 μg/1 μl of Ratiometric-pericam-mt/pcDNA3 was added to 199 μl Opti-MEM (Invitrogen, Carlsbad, CA), and 1 μl Lipofectamine 2000 (Invitrogen, Carlsbad, CA) was added to 9 μl Opti-MEM. Both solutions were incubated separately at room temperature for 5 min, mixed and then incubated at room temperature for an additional 15–20 min. Meanwhile, serum-containing medium was removed from cells and replaced with 1 ml of Opti-MEM for 30 min. Opti-MEM was then removed and replaced with 800 μl of fresh Opti-MEM to which 200 μl of the Ratiometric-pericam-mt/pcDNA3 solution had been added. Cells were then incubated at 37 °C in a 5% CO_2 atmosphere for 4 h to initiate transfection. Then, 500 μl DMEM supplemented with 5% FBS was added to each well to maintain cell viability. 96 h later, cells were perfused with normal Tyrode's solution at 37 °C. When Ca^{2+} fluorescence levels reached a steady state, 10 μM ATP was applied for 10 s through a small perfusion pipe. Dual-excitation imaging with Ratiometric-pericam-mt required two filters (EX:482/35, DM:506, EM:536/40 and EX:414/46, DM:510, EM:527/20). Changes in ATP-induced Ca^{2+} release from the SR to mitochondria were determined using a Metafluor Imaging system (Molecular Devices, Sunnyvale, CA).

2.7. Measurement of ATP content

ATP measurement was performed using an ATP assay kit (Toyo Ink, Tokyo, Japan), according to the manufacturer's protocol. Briefly, frozen Neuro2a cells were homogenized in homogenate buffer (0.25 M sucrose and 10 mM HEPES–NaOH, pH 7.4), and lysates were cleared by centrifugation at 1000 g for 10 min at 4 °C. The supernatant was collected, and supernatant proteins were solubilized in extraction buffer. After 30 min, luciferin buffer was added to each sample and oxyluciferin was detected using a luminometer (Gene Light 55, Microtec, Funabashi, Japan).

2.8. Measurement of proteasome activity

Proteasome activity was measured according to Thomas et al. with some modifications [25]. Briefly, cells were lysed in PBS containing 0.1% Triton X-100 and 0.5 mM DTT. Lysates were diluted in assay buffer (25 mM HEPES, pH 7.5, 0.5 mM EDTA, 0.05% NP-40 and 0.001% SDS) containing 200 μM Suc-LLVY-AMC (EMD-Calbiochem, La Jolla, CA). After a 1-hour incubation at 37 °C, fluorescence of free AMC was measured using excitation and emission wavelengths of 355 and 460 nm, respectively.

2.9. TUNEL staining

DNA fragmentation and apoptotic bodies were detected by TUNEL staining using an *in situ* apoptosis detection kit (Takara Bio Inc., Shiga, Japan), as described in [18].

2.10. Statistical analysis

Values are represented as means ± standard error of the mean (S.E.M.). Results were evaluated for differences using one-way ANOVA, followed by multiple comparisons using Dunnett's test. $P < 0.05$ was considered statistically significant.

3. Results

3.1. A missense mutation promotes aberrant intracellular distribution of σ_1R protein

To compare intracellular distribution of wild-type σ_1R with that of σ_1R^{E102Q}, we investigated localization of mCherry-tagged σ_1R (σ_1R-mCherry) or σ_1R^{E102Q} (σ_1R^{E102Q}-mCherry) after overexpression of each in Neuro2A cells. At 48 h after transfection, both proteins showed similar cytoplasmic distribution, whereas by 96 h, σ_1R^{E102Q} became aggregated in the cytoplasm, while σ_1R remained evenly distributed in the cytoplasm (Fig. 1A). We next asked which organelles contained aggregated σ_1R^{E102Q} at the 96 h time point. Wild-type σ_1R co-localized primarily with the ER marker SERCA (Fig. 1B) and in part with the Golgi marker GM130 (Fig. 1C). Aggregated σ_1R^{E102Q}, however, did not co-localize with SERCA and GM130. Native σ_1R localizes to the mitochondria-associated ER membrane (MAM); thus, σ_1R-mCherry co-localized with the mitochondrial protein cytochrome *c*, while σ_1R^{E102Q}-mCherry did not co-localize with cytochrome *c* (Fig. 1D). We also investigated whether σ_1R^{E102Q}-mCherry localized to proteasomes or autophagosomes, both of which function in protein degradation. Large σ_1R^{E102Q}-mCherry aggregates co-localized partly with the proteasome (Fig. 1E), but not with the autophagosome based on analysis of the marker LC3 (Fig. 1F); by contrast, σ_1R-mCherry was not associated with either proteasomes or autophagosomes (Fig. 1E). These results suggest that σ_1R^{E102Q} gradually dissociates from ER membranes, undergoes aggregation, and is then transported to cytoplasmic proteasomes.

3.2. σ_1R^{E102Q} expression decreases IP_3R-mediated mitochondrial Ca^{2+} mobilization and ATP production and impairs proteasome activity

We next investigated σ_1R function in the MAM. The σ_1R/IP_3R complex is critical for ER–mitochondrial Ca^{2+} transport, as reported by Hayashi and Su [17]. To assay mitochondrial Ca^{2+} transport in Neuro2A cells expressing non-tagged σ_1R or σ_1R^{E102Q}, we conducted mitochondrial Ca^{2+} imaging using a Ratiometric-pericam-mt Ca^{2+} probe, which localizes to mitochondria and is an indicator of mitochondrial Ca^{2+} mobilization [24]. To evaluate IP_3R-mediated mitochondrial Ca^{2+} influx, we stimulated cells with ATP, which acts on a Gq-coupled receptor. Compared with non-transfected cells, σ_1R-transfected cells showed significantly increased ATP-induced mitochondrial Ca^{2+} transport, whereas σ_1R^{E102Q}-transfected cells showed decreased transport relative to non-transfected control cells ($P < 0.01$ *vs.* control) (Fig. 2A–C).

IP_3R-mediated Ca^{2+} transport into mitochondria promotes oxidative phosphorylation, mitochondrial respiratory chain activity and subsequent ATP production by activating the TCA cycle [26]. Indeed, IP_3R-mediated Ca^{2+} transport into mitochondria promotes ATP production in Neuro2A cells [18]. Thus, we asked whether σ_1R^{E102Q} impairs mitochondrial ATP production. Consistent with our previous observation [18], σ_1R overexpression significantly enhanced ATP production, whereas ATP production decreased in σ_1R^{E102Q}-overexpressing cells relative to non-transfected control cells (Fig. 2D). ER stress induced by 48 h of tunicamycin treatment caused markedly reduced ATP production. σ_1R overexpression significantly inhibited tunicamycin-induced ATP reduction, whereas σ_1R^{E102Q} overexpression failed to rescue it (Fig. 2D). We also confirmed that impaired mitochondrial Ca^{2+} transport caused by treatment with Ru360, an inhibitor of the mitochondrial Ca^{2+} uniporter (MCU), markedly reduced ATP levels in both control and

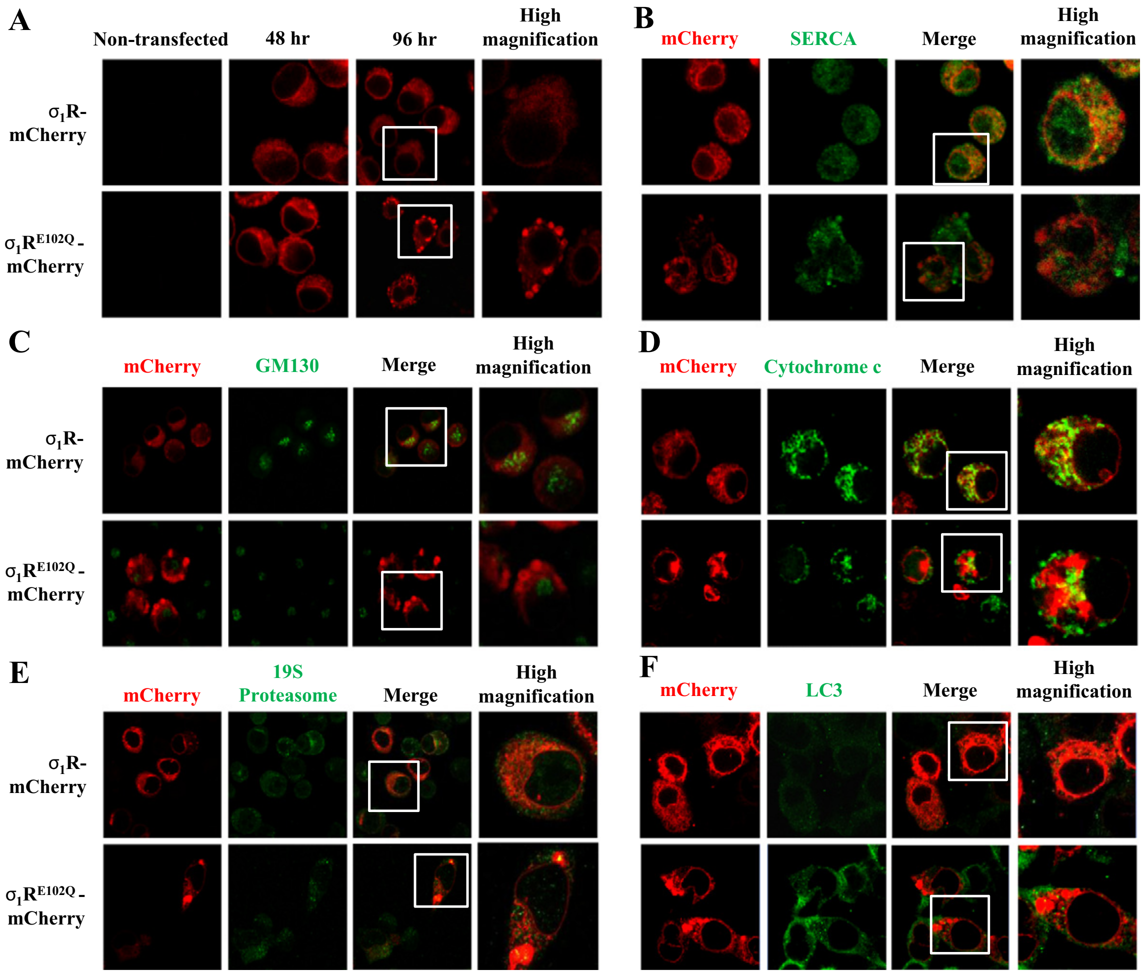

Fig. 1. Intracellular localization of overexpressed σ_1R- or σ_1R^{E102Q}-mCherry proteins in transfected Neuro2A cells. (A) Immunofluorescence showing intracellular localization of σ_1R or σ_1R^{E102Q} (red). (B–F) Immunofluorescence showing intracellular localization of σ_1R or σ_1R^{E102Q} (red) and the Golgi marker GM130 (green) (B), the ER marker SERCA (green) (C), the mitochondrial marker cytochrome *c* (green) (D), the 19S proteasome marker (green) (E) or the autophagy marker LC3 (green) (F).

ER stress conditions, similar to σ_1R^{E102Q} overexpression (Fig. 2D). Treatment of σ_1R^{E102Q}-overexpressing cells with Ru360 did not elicit further ATP reduction. More importantly, ATP supplementation through treatment with methyl pyruvate (MP), a substrate in the mitochondrial TCA cycle, significantly rescued ATP reduction brought on by σ_1R^{E102Q} overexpression, with or without tunicamycin treatment (Fig. 2D).

Both ubiquitination and proteasomal degradation are ATP-dependent activities, and prolonged ER stress impairs the UPS [27,28]. Moreover, Neuro2A cells stably expressing a mutant and misfolded form of SOD1 show decreased proteasome activity [29]. Thus, we evaluated proteasome activity 96 h after σ_1R^{E102Q} transfection (Fig. 2E). As expected, σ_1R^{E102Q} overexpression decreased proteasome activity and exacerbated impaired proteasome activity brought on by tunicamycin treatment. Consistent with observations shown in Fig. 2D, Ru360 treatment markedly decreased proteasome activity either with or without ER stress (Fig. 2E). Furthermore, aberrant proteasome activity induced by σ_1R^{E102Q} overexpression, either alone or with tunicamycin treatment, was ameliorated by MP treatment, as expected.

3.3. Overexpressed σ_1R^{E102Q}, but not σ_1R, gradually dissociates from IP_3R3 to form cytoplasmic aggregates

Impaired mitochondrial Ca^{2+} transport and ATP production may be due to the loss of σ_1R^{E102Q}/IP_3R binding capacity. Thus, we investigated association of σ_1R or σ_1R^{E102Q} with the IP_3R3, the predominant IP_3R isoform expressed in Neuro2A cells. Immunoprecipitation with an IP_3R3 antibody was carried out in lysates collected at 48 or 96 h after transfection, followed by detection of 55 kDa σ_1R-mCherry or σ_1R^{E102Q}-mCherry. Consistent with our previous report [18], both σ_1R-mCherry and σ_1R^{E102Q}-mCherry were associated with the IP_3R3 at 48 h after transfection (Fig. 3A), but the association of σ_1R^{E102Q} with IP_3R3 significantly decreased by 96 h, a decrease not seen with the wild-type protein (Fig. 3B, C). These results suggest that, unlike the wild-type protein, σ_1R^{E102Q} mutant protein slowly dissociates from the IP_3R3.

3.4. σ_1R^{E102Q} enhances autophagic cell death under ER stress conditions

Al-Saif et al. reported that a mouse motor neuron-like cell line is less resistant to apoptosis induced by ER stress following σ_1R^{E102Q} transfection [13]. Based on these observations, we hypothesized that σ_1R^{E102Q} causes autophagic cell death. To test this, we examined expression of LC3-II, a marker of autophagy, in cells transfected with mutant and wild-type forms of σ_1R with or without tunicamycin treatment. Significantly, we observed that the ratio of LC3-II to total (LC3-I plus LC3-II) LC3 markedly increased in σ_1R^{E102Q}-transfected and tunicamycin-treated cells at 48 h after tunicamycin treatment. The LC3-II/total LC3 ratio slightly but significantly increased after σ_1R^{E102Q} overexpression under basal conditions without ER stress (Fig. 4A, B). Treatment with MP (5 μM) for the last 48 h significantly inhibited the σ_1R^{E102Q} overexpression-related increase in the LC3-II/total LC3 ratio (Fig. 4B) and tended to suppress tunicamycin- and σ_1R^{E102Q} overexpression-

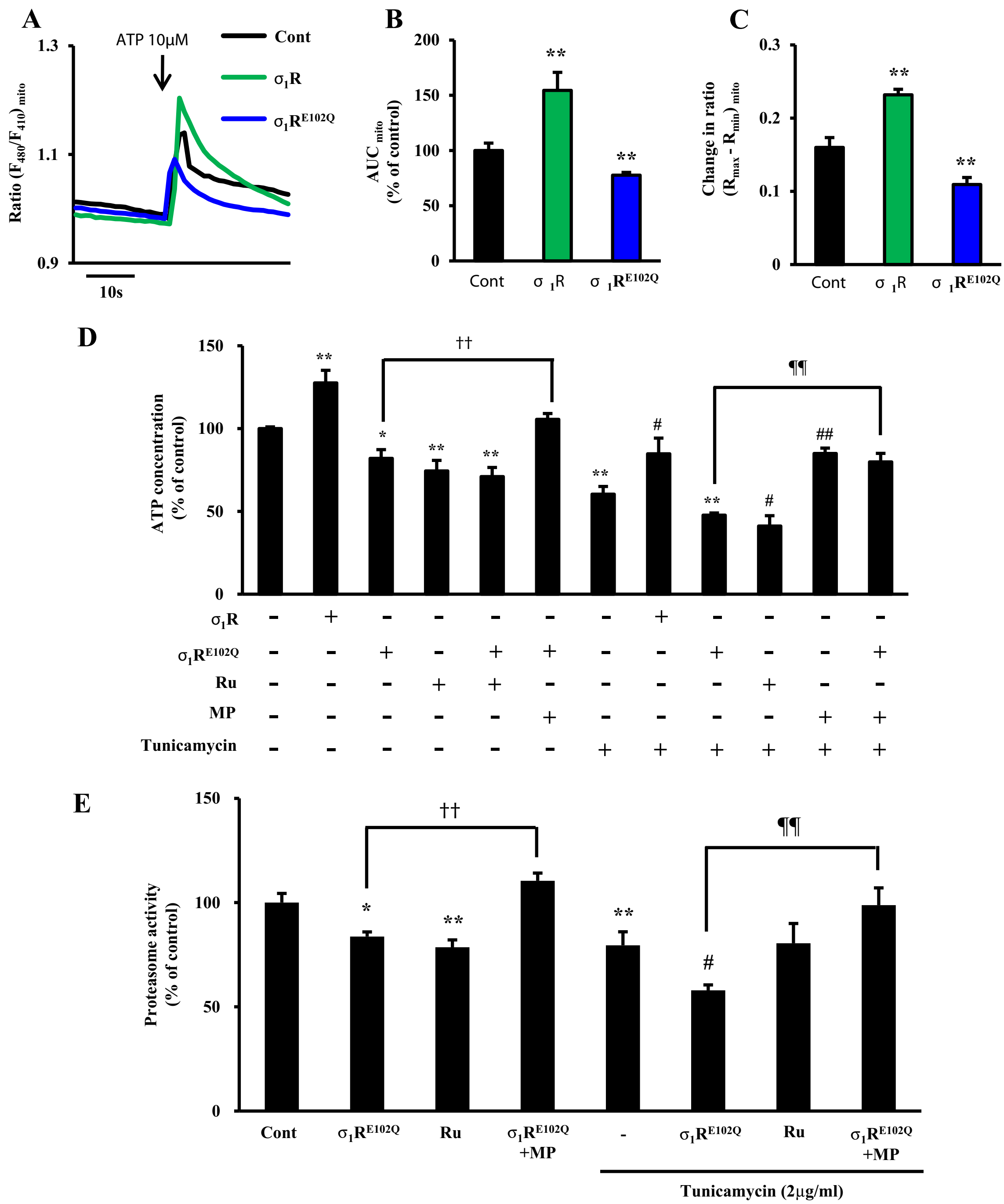

Fig. 2. Effects of σ_1R or σ_1R^{E102Q} transfection on ATP-induced Ca^{2+} mobilization to mitochondria, on mitochondrial ATP content and on proteasome activity in Neuro2A cells. (A) Time courses of ATP-induced Ca^{2+} influx into mitochondria. (B) Area under the curve (AUC) quantification of ATP-induced Ca^{2+} influx into mitochondria and (C) peak increases in $[Ca^{2+}]_{mito}$. Each group consists of greater than 10 cells. (D) Measurement of cellular ATP content with or without tunicamycin (2 μg/ml), MP (5 μM) or Ru360 (10 μM) for 48 h. (E) Measurement of proteasome activity with or without tunicamycin, MP or Ru360 for 48 h. Each column represents the mean ± S.E.M. *, $P < 0.05$ and **, $P < 0.01$ *versus* control cells; #, $P < 0.05$ and ##, $P < 0.01$ *versus* tunicamycin-treated cells; ††, $P < 0.01$ *versus* σ_1R^{E102Q}-transfected cells; ¶¶, $P < 0.01$ *versus* σ_1R^{E102Q}-transfected and tunicamycin-treated cells.

induced autophagy (Fig. 4B). σ_1R overexpression blocked tunicamycin-induced LC3-II induction (Fig. 4A, B). We next confirmed LC3 accumulation by immunocytochemistry and assessed mitochondrial membrane potential using MitoTracker Red CMXRos (MitoTracker) staining. LC3 immunoreactivity appeared in a diffuse pattern in non-transfected and wild-type σ_1R-transfected cells (Fig. 4C). In contrast, accumulation of LC3-positive particles indicative of autophagosomes slightly increased in both σ_1R^{E102Q}-transfected and tunicamycin-treated cells. σ_1R^{E102Q}-transfected cells that were also treated with tunicamycin showed markedly enhanced LC3 accumulation (Fig. 4C). Conversely, mitochondrial membrane potential as assessed by MitoTracker slightly decreased following σ_1R^{E102Q} transfection or tunicamycin treatment and markedly decreased after 48 h in σ_1R^{E102Q} transfected and tunicamycin treated cells (Fig. 4C). As expected, overexpression of wild-type σ_1R inhibited tunicamycin-induced LC3 accumulation and restored mitochondrial membrane potential, as assessed by MitoTracker fluorescence (Fig. 4C).

Since interactions between autophagic and apoptotic processes have been documented [30], we confirmed differing effects of σ_1R and σ_1R^{E102Q} overexpression on apoptotic cell death using TUNEL staining.

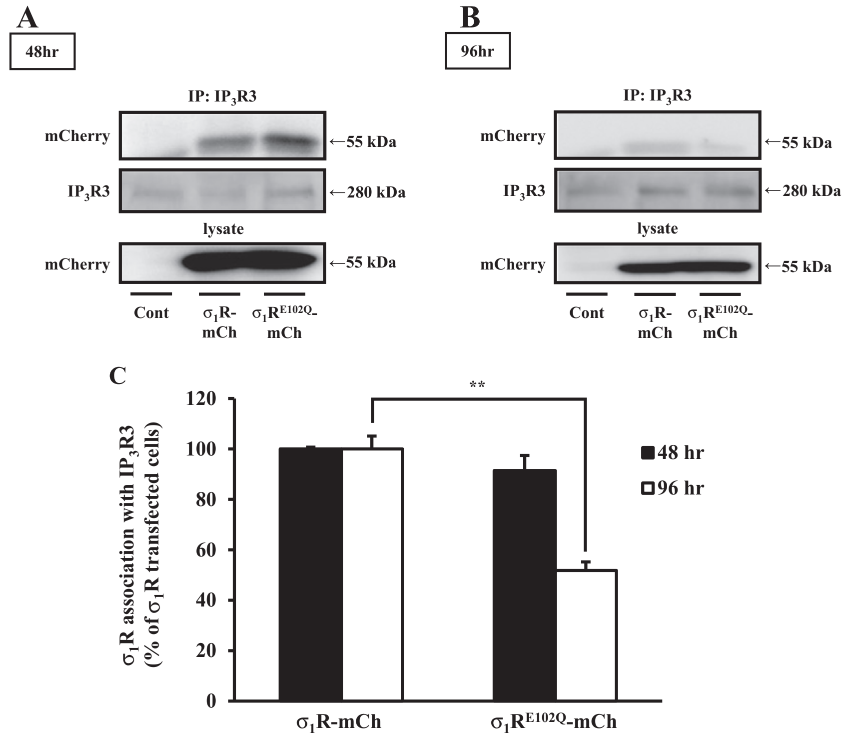

Fig. 3. Interaction of σ_1R or σ_1R^{E102Q} with the IP_3R3 in Neuro2A cells. (A) Immunoprecipitation analysis of σ_1R or IP_3R3 in lysates of cells with or without transfection. At 48 h after σ_1R-mCherry or σ_1R^{E102Q}-mCherry transfection, lysate proteins were immunoprecipitated with an anti-IP_3R3 antibody. Immunocomplexes were separated on SDS-PAGE and immunoblotted using anti-DsRed antibody. (B) Immunoprecipitation analysis of σ_1R or IP_3R3 in lysates of cells with or without transfection. At 96 h after σ_1R-mCherry or σ_1R^{E102Q}-mCherry transfection, lysate proteins were immunoprecipitated with an anti-IP_3R3 antibody. (C) Densitometry quantification of σ_1R-mCherry/IP_3R3 association at either 48 or 96 h after σ_1R or σ_1R^{E102Q} transfection. Each column represents the mean ± S.E.M. **, $P < 0.01$ *versus* σ_1R-mCherry-expressing cells 48 h after transfection.

Tunicamycin treatment of non-transfected cells for 48 h significantly induced apoptosis, as indicated by the increased number of TUNEL-positive cells compared to untreated cells ($P < 0.01$ *vs.* control) (Fig. 4D). σ_1R^{E102Q} overexpression also induced apoptosis of normal cells with or without tunicamycin treatment. σ_1R overexpression partially but significantly inhibited tunicamycin-induced apoptosis by 48 h tunicamycin treatment ($P < 0.01$ *vs.* tunicamycin) (Fig. 4D). Conversely, σ_1R^{E102Q} overexpression significantly enhanced tunicamycin-induced apoptosis ($P < 0.05$ *vs.* tunicamycin) (Fig. 4D). Treatment with MP (5 μM) for the last 48 h significantly inhibited σ_1R^{E102Q} overexpression-induced apoptosis without tunicamycin (Fig. 4D). Treatment of tunicamycin-treated cells with 3-methyladenine (3-MA), an inhibitor of autophagy, significantly inhibited tunicamycin-induced apoptosis ($P < 0.01$ *vs.* tunicamycin) (Fig. 4D). In addition, σ_1R^{E102Q} overexpression-induced apoptosis was also inhibited by 3-MA treatment ($P < 0.05$ *vs.* σ_1R^{E102Q} transfected cells) (Fig. 4D). These data suggest that σ_1R^{E102Q} overexpression induces autophagy and enhances ER stress-induced apoptosis.

3.5. σ_1R^{E102Q} overexpression promotes degradation of mitochondrial proteins without effects on ER–mitochondrial junctional proteins

Since mitochondrial membrane potential was markedly reduced following ER stress in σ_1R^{E102Q}-overexpressing cells, we hypothesized that ATP reduction caused by dissociation of σ_1R from the MAM triggers mitochondrial degradation. To assess this, we evaluated expression levels of proteins localizing at the MAM and mitochondria. Following σ_1R^{E102Q} overexpression, we observed slightly reduced levels of mitochondria-associated proteins such as VDAC and mitofusin 1 (Mfn 1) (Fig. 5A–C), reductions that were enhanced following ER stress (Fig. 5A–C). However, levels of proteins that mediate ER–mitochondria linkage such as GRP75 and mitofusin 2 (Mfn 2) were unchanged (Fig. 5A). Since both GRP75 and Mfn2 localize to the ER membrane [31,32], mitochondrial degradation may precede degradation of other cellular organelles such as the ER when σ_1R^{E102Q} is overexpressed. Levels of endogenous σ_1R were downregulated by σ_1R^{E102Q} overexpression and treatment with tunicamycin alone, as well as a combination of the two (Fig. 5A, D).

Since σ_1R^{E102Q} dissociation from the ER and its aggregation may promote ER stress, we assessed signals of ER stress, including PERK and IRE1 phosphorylation and induction of ATF6 protein. Indeed, 48 h of tunicamycin treatment significantly increased PERK phosphorylation in non-transfected cells, although IRE1 phosphorylation and ATF6 protein levels remained unchanged (Fig. 5A). However, σ_1R^{E102Q} overexpression had no effect on PERK and IRE1 phosphorylation or ATF6 protein levels (Fig. 5A). Total PERK and IRE1 expression also remained unchanged among groups (Fig. 5A), suggesting that slow dissociation of σ_1R^{E102Q} proteins from ER membranes and their accumulation in the cytoplasm does not trigger ER stress. Also, impairment of proteasome activity by σ_1R^{E102Q} overexpression might be insufficient to induce ER stress.

To confirm that reduced ATP production triggers mitochondrial damage, we asked whether σ_1R^{E102Q}-induced ATP depletion preceded mitochondrial degradation. At 72 h after σ_1R^{E102Q} transfection, ATP content significantly decreased (Fig. 5F), while expression levels of each protein were unchanged compared to non-transfected cells (Fig. 5E), suggesting that mitochondrial dysfunction precedes degradation of mitochondrial proteins such as VDAC and Mfn 1.

3.6. σ_1R^{E102Q} enhances extra-nuclear localization of an ALS-associated DNA binding protein

The trans-activating response (TAR) element DNA binding protein (TDP-43), a predominantly nuclear 414 amino acid protein, exhibits an N-terminal nuclear localization signal and a nuclear export signal in its middle region. Dominant mutations in *TARDBP* seen in patients

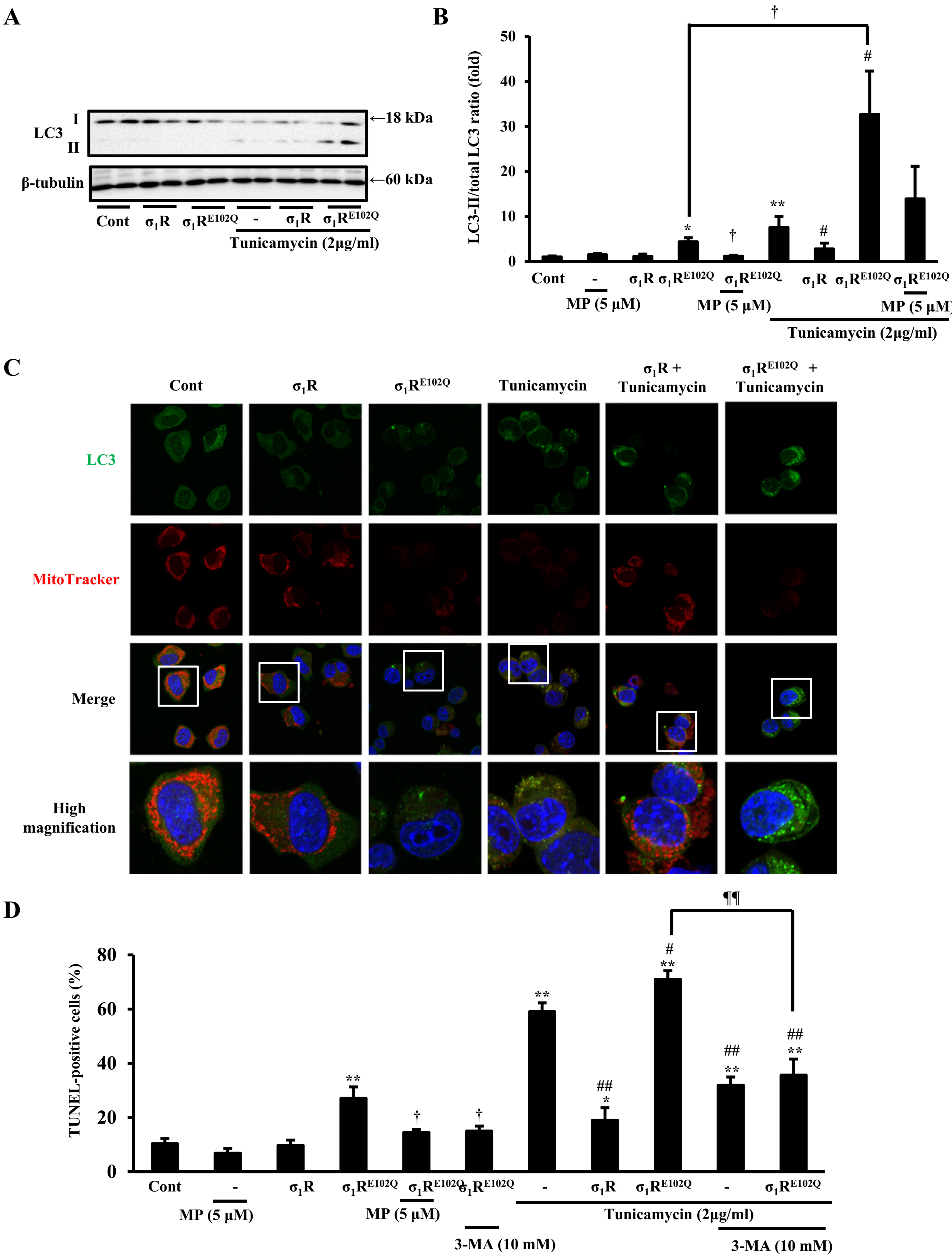

Fig. 4. Effects of σ_1R or σ_1R^{E102Q} transfection and tunicamycin treatment on autophagy in Neuro2A cells. (A) Western blot analysis of LC3-I and LC3-II expression in cells treated with or without tunicamycin for 48 h. (B) Densitometry quantification of LC3-I and LC3-II in cells treated with or without tunicamycin for 48 h. Data are expressed as a ratio of LC3-II to total LC3 (LC3-I plus LC3-II). Control cell ratios are also shown. (C) Confocal analysis of LC3 and MitoTracker Red in cells treated with or without tunicamycin for 48 h. (D) Quantitative analysis of apoptotic cells based on TUNEL staining of σ_1R- or σ_1R^{E102Q}-transfected cells in different treatment conditions. Each column represents the mean ± S.E.M. *, $P < 0.05$ and **, $P < 0.01$ *versus* control cells; #, $P < 0.05$ and ##, $P < 0.01$ *versus* tunicamycin-treated cells; †, $P < 0.05$ *versus* σ_1R^{E102Q}-transfected cells; ¶¶, $P < 0.01$ *versus* σ_1R^{E102Q}-transfected and tunicamycin-treated cells.

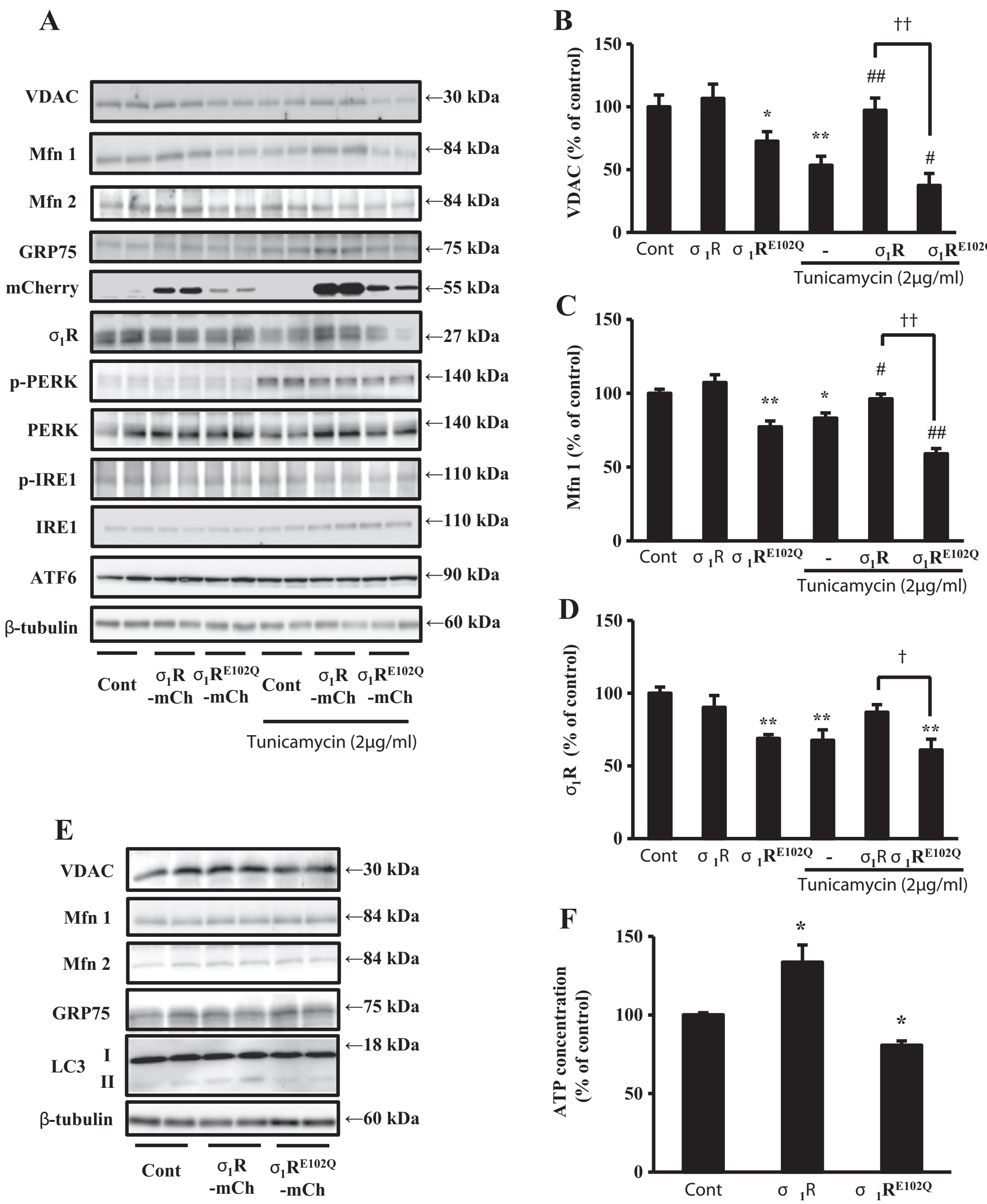

Fig. 5. Effects of σ_1R or σ_1R^{E102Q} transfection and tunicamycin treatment on mitochondrial degradation and ER stress in Neuro2A cells. (A) Representative immunoblots probed with various antibodies are shown in control, σ_1R-mCherry- or σ_1R^{E102Q}-mCherry-expressing cells treated with or without 2 μg/ml tunicamycin for 48 h. (B–D) Densitometry quantification of each protein in cells treated with or without tunicamycin for 48 h. (E) Representative immunoblots probed with various antibodies are shown in control, σ_1R-mCherry- or σ_1R^{E102Q}-mCherry-expressing cells 72 h after transfection. (F) Measurement of cellular ATP content in control, σ_1R- or σ_1R^{E102Q}-expressing cells 72 h after transfection. Data are expressed as percentages of the value of control cells. Each column represents the mean ± S.E.M. *, $P < 0.05$ and **, $P < 0.01$ *versus* control cells; #, $P < 0.05$ and ##, $P < 0.01$ *versus* tunicamycin-treated cells; †, $P < 0.05$ and ††, $P < 0.01$ *versus* σ_1R-transfected and tunicamycin-treated cells.

with familial ALS promote cytoplasmic accumulation and aggregation of mutant protein in spinal cord motor neurons [10]. In ALS, TDP-43 protein also exhibits enhanced ubiquitination, phosphorylation and fragmentation [10]. Since nuclear transport and proteasome degradation are ATP-dependent [27,33–35], we hypothesized that nuclear localization and degradation of ubiquitinated TDP-43 could be impaired following σ_1R^{E102Q} overexpression. To test this hypothesis, we evaluated TDP-43 localization and ubiquitination in the presence or absence of ER stress. σ_1R^{E102Q} overexpression for 96 h impaired TDP-43 nuclear localization, an effect not seen following σ_1R overexpression (Fig. 6A, D). Moreover, overexpressed σ_1R^{E102Q} aggregated in the cytoplasm. Interestingly, tunicamycin treatment for the last half of the 96-hour incubation enhanced cytoplasmic TDP-43 localization in σ_1R^{E102Q}-overexpressing cells and promoted formation of aggregated inclusion bodies in both the nucleus and cytoplasm (Fig. 6A, D). Conversely, σ_1R overexpression prevented tunicamycin-induced cytoplasmic mislocalization and TDP-43 aggregation (Fig. 6A, D). However, TDP-43 immunoreactive protein did not show aggregated patterns seen with σ_1R^{E102Q}-mCherry immunoreactive proteins (Fig. 6A), suggesting that σ_1R^{E102Q} does not co-aggregate with TDP-43. To confirm that proteasome impairment accounts for TDP-43 cytoplasmic mislocalization, we treated cells with the potent proteasome inhibitor MG132. MG132 treatment triggered the cytoplasmic TDP-43 mislocalization, an effect enhanced in the presence of tunicamycin

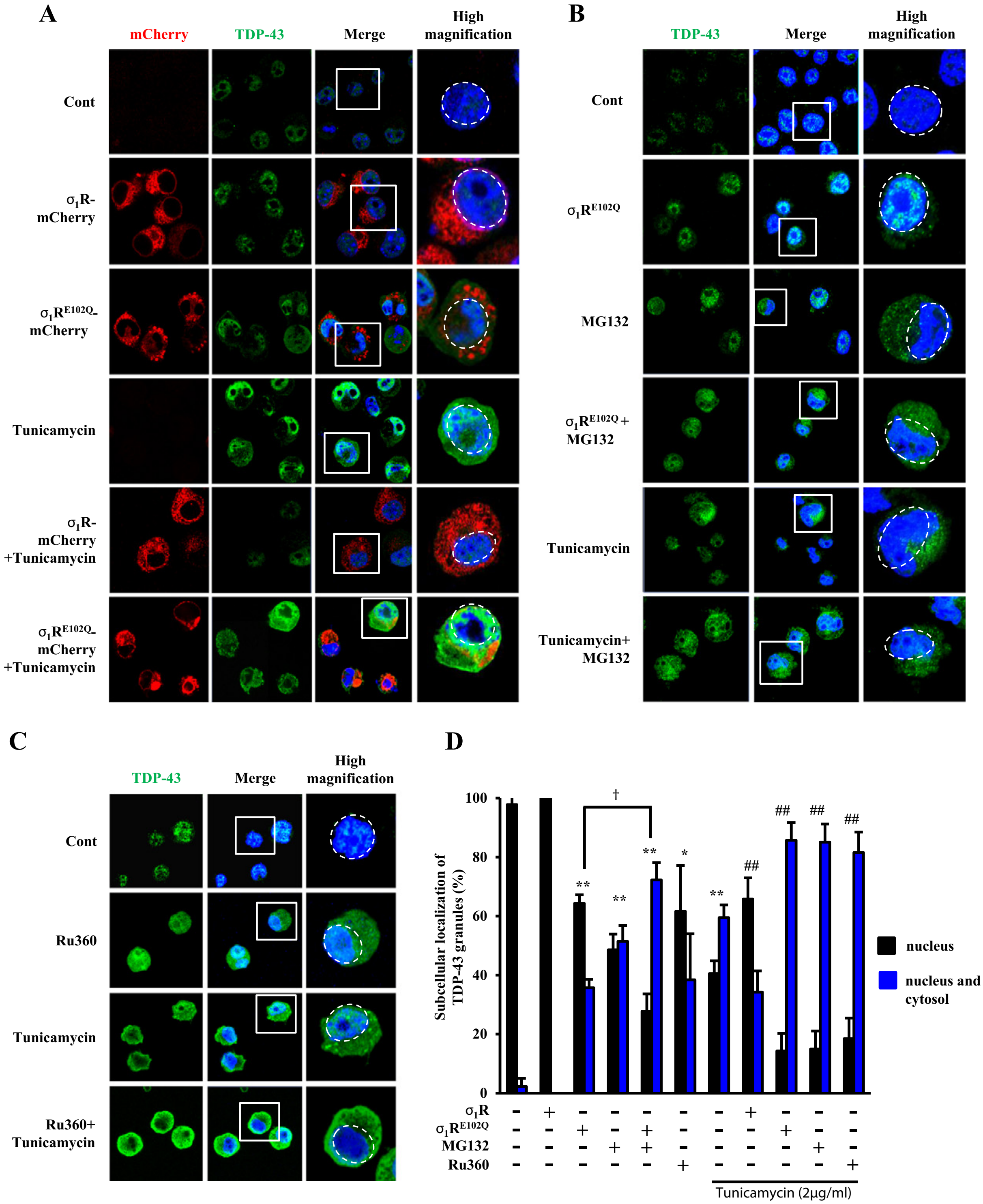

Fig. 6. Effect of tunicamycin treatment, σ_1R^{E102Q} overexpression or Ru360 treatment on TDP-43 mislocalization. (A) Confocal analysis of σ_1R or σ_1R^{E102Q} (red), TDP-43 (green) and DAPI (blue) in Neuro2A cells with or without tunicamycin (2 μg/ml, 48 h). Dashed circles show nuclei stained by DAPI. (B) Confocal analysis of TDP-43 (green) and DAPI (blue) in cells treated with or without MG132 for 48 h. (C) Confocal analysis of TDP-43 (green) and DAPI (blue) in cells treated with or without Ru360 for 48 h. (D) Quantification of cells showing nuclear or cytoplasmic TDP-positivity. Data are expressed as percentages of the total cell number. Each group consists of greater than 35 cells. Each column represents the mean ± S.E.M. *, $P < 0.05$ and **, $P < 0.01$ *versus* control cells; ##, $P < 0.01$ *versus* tunicamycin-treated cells; †, $P < 0.05$ *versus* σ_1R^{E102Q}-transfected cells.

or σ_1R^{E102Q} transfection (Fig. 6B, D). To confirm that both impaired mitochondrial Ca^{2+} transport and ATP reduction account for TDP-43 cytoplasmic mislocalization, we treated cells with mitochondrial Ca^{2+} transport inhibitor Ru360. As expected, Ru360 treatment triggered cytoplasmic TDP-43 mislocalization, and in fact aggravated it in the presence of tunicamycin (Fig. 6C, D).

To further evaluate extra-nuclear TDP-43 localization, we counted cells showing either nuclear or extra-nuclear TDP-43 localization. Without tunicamycin treatment, σ_1R^{E102Q} overexpression or Ru360 treatment triggered extra-nuclear TDP-43 localization, and both conditions enhanced tunicamycin-induced extra-nuclear localization (Fig. 6D). On the other hand, σ_1R overexpression significantly inhibited tunicamycin-induced extra-nuclear TDP-43 localization (Fig. 6D).

3.7. ATP supplementation rescues σ_1R^{E102Q}-induced anomalous TDP-43 distribution following ER stress

We next asked whether ATP supplementation by MP treatment would inhibit aberrant cytoplasmic localization of TDP-43. To do so, we treated wild-type or σ_1R^{E102Q}-overexpressing Neuro 2A cells with MP (5 μM) or tunicamycin plus MP for 48 h. MP treatment inhibited extra-nuclear localization of TDP-43 seen in both σ_1R^{E102Q}-overexpressing cells and σ_1R^{E102Q}-overexpressing plus tunicamycin-treated cells (Fig. 7A, B). These results suggest that the reduced ATP synthesis and impaired proteasomal function promoted by σ_1R^{E102Q} overexpression likely promotes TDP-43 mislocalization.

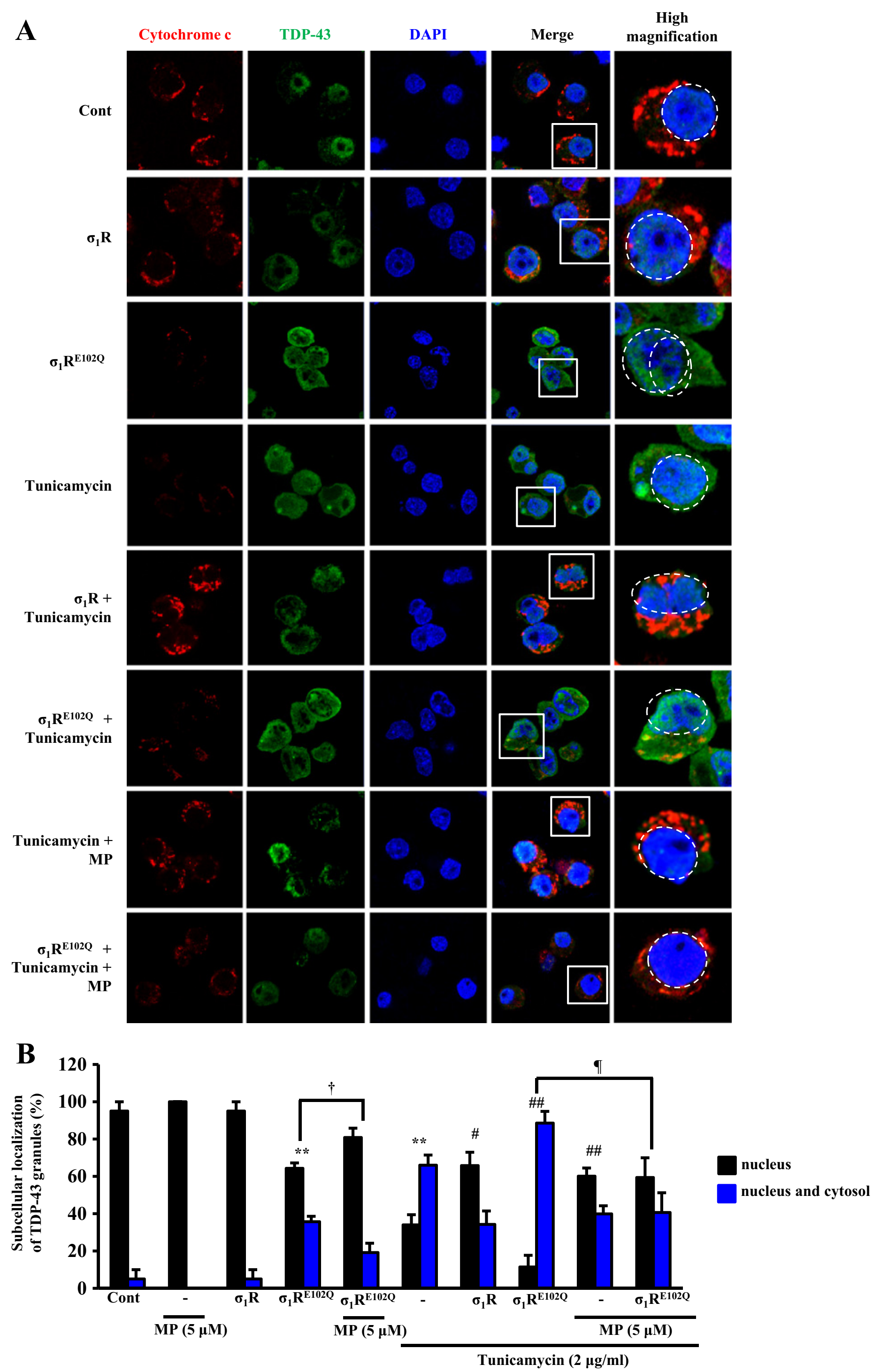

Fig. 7. ATP supplementation inhibits σ_1R^{E102Q}-induced TDP-43 mislocalization. (A) Confocal analysis of σ_1R or cytochrome *c* (red), TDP-43 (green) and DAPI (blue) in Neuro2A cells with or without tunicamycin (2 μg/ml, 48 h) or MP (5 μM, 48 h) treatment. Dashed circles show nuclei stained by DAPI. (B) Quantification of cells showing nuclear or cytoplasmic TDP-positivity. Data are expressed as percentages of the total cell number. Each group consists of greater than 35 cells. Each column represents the mean ± S.E.M. **, $P < 0.01$ *versus* control cells; #, $P < 0.05$ and ##, $P < 0.01$ *versus* tunicamycin-treated cells; †, $P < 0.05$ *versus* σ_1R^{E102Q}-transfected cells; ¶, $P < 0.05$ *versus* σ_1R^{E102Q}-transfected and tunicamycin-treated cells.

We also investigated mitochondrial morphology 48 h after transfection using the mitochondrial marker cytochrome *c*, whose localization is independent of mitochondrial membrane potential. Mitochondrial size decreased by 48 h after tunicamycin treatment, suggestive of mitochondrial degradation (Fig. 7A). Mitochondrial size also decreased relative to non-transfected cells in basal conditions seen following σ_1R^{E102Q} overexpression (Fig. 7A). Interestingly, σ_1R overexpression inhibited tunicamycin-induced mitochondrial degradation, but σ_1R^{E102Q} overexpression promoted mitochondrial degradation under ER stress conditions (Fig. 7A). These results suggest that σ_1R^{E102Q} aggregation contributes to mitochondrial dysfunction and ATP depletion, leading to abnormal TDP-43 distribution under ER stress conditions.

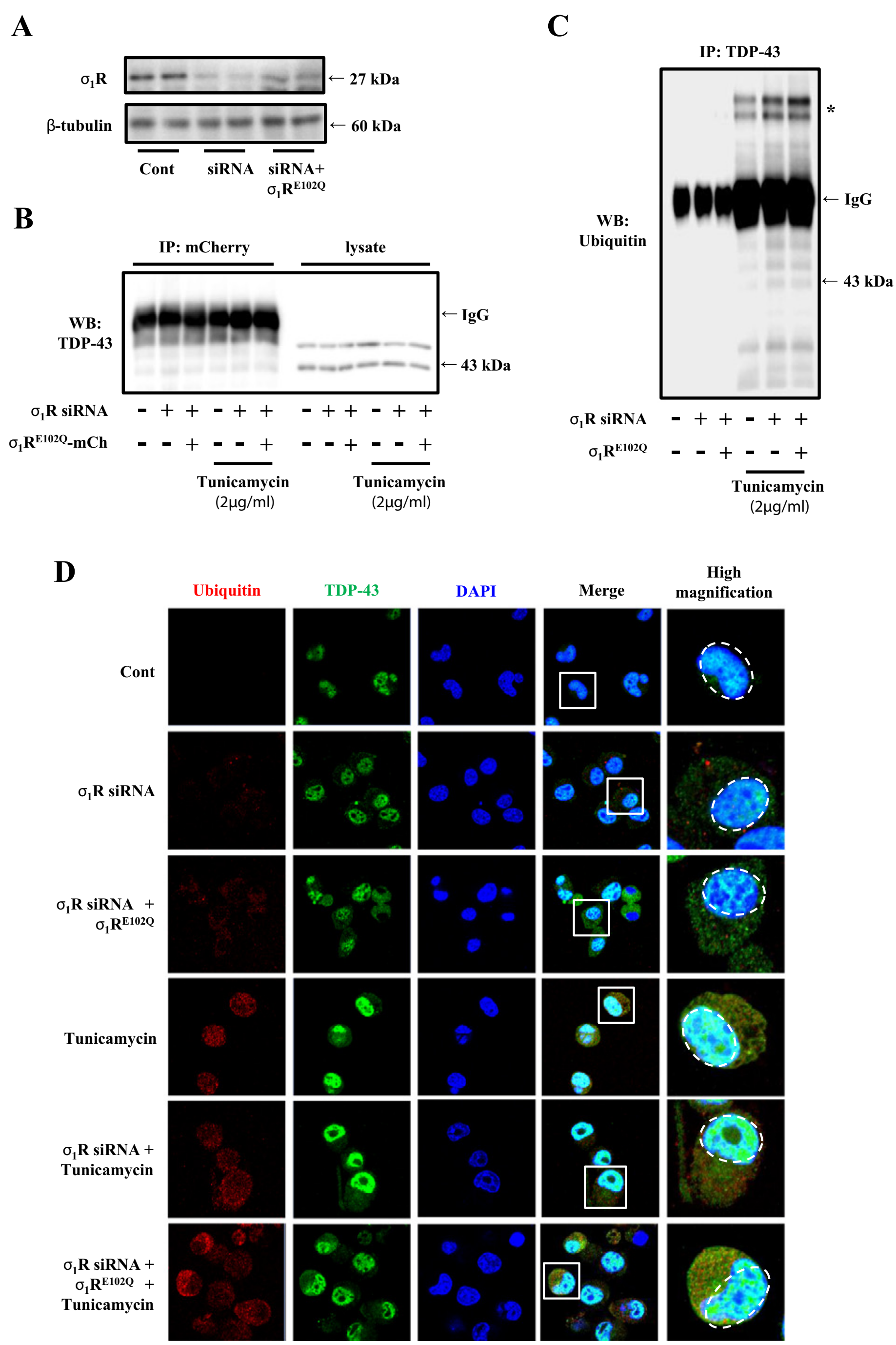

Fig. 8. siRNA σ_1R knockdown increases tunicamycin-induced TDP-43 ubiquitination. (A) Western blot analysis of σ_1R expression in cells treated with or without σ_1R siRNA and/or σ_1R^{E102Q} transfection. (B) Immunoprecipitation analysis of σ_1R^{E102Q}-mCherry and TDP-43 in lysates of cells with or without transfection. At 96 h after σ_1R or σ_1R^{E102Q} transfection, lysate proteins were immunoprecipitated with an anti-DsRed polyclonal antibody. Immunocomplexes were separated on SDS-PAGE and immunoblotted using an anti-TDP-43 antibody. (C) Effects of siRNA-mediated σ_1R knockdown, σ_1R^{E102Q} transfection and tunicamycin treatment on TDP-43 ubiquitination in Neuro2A cells. Ubiquitination was assayed at 48 h after transfection and drug treatment when applicable. After immunoprecipitation with an anti-TDP-43 antibody, immunoprecipitants were separated on SDS-PAGE and immunoblotted using an anti-ubiquitin antibody. (D) Confocal analysis of ubiquitin (red), TDP-43 (green) and DAPI (blue) in non-transfected, σ_1R siRNA- or σ_1R^{E102Q}-transfected cells 96 h after transfection with or without tunicamycin (2 μg/ml, 48 h) treatment.

3.8. siRNA-mediated σ_1R knockdown aggravates tunicamycin-induced TDP-43 ubiquitination

The extra-nuclear localized TDP-43 did not merge with σ_1R^{E102Q} aggregates (Fig. 6A). Therefore, we confirm whether σ_1R^{E102Q} binds to TDP-43 using immunoprecipitation combined with σ_1R siRNA treatment. Endogenous σ_1R levels were significantly reduced by siRNA treatment (Fig. 8A), and immunoprecipitation using a mCherry antibody following expression of σ_1R^{E102Q}-mCherry did not pull down TDP-43 (Fig. 8B). Thus, neither endogenous σ_1R nor expressed σ_1R^{E102Q} formed a complex with TDP-43, a finding consistent with their subcellular distribution. Furthermore, to confirm whether σ_1R knockdown by siRNA alters tunicamycin-induced TDP-43 ubiquitination, we probed Western blots of immunoprecipitates with a TDP-43 antibody. We did not detect ubiquitinated TDP-43 in the absence of tunicamycin-dependent ER stress. When endogenous σ_1R was knocked down by σ_1R siRNA, tunicamycin-induced TDP-43 ubiquitination increased, as evidenced by the appearance of multiple higher molecular weight species on SDS-PAGE. σ_1R^{E102Q} expression further enhanced ubiquitination of TDP-43 (see bands marked by the asterisk in Fig. 8C). Immunocytochemical analysis also confirmed increased TDP-43 ubiquitination (Fig. 8D). Interestingly, σ_1R knockdown itself induced mild extra-nuclear TDP-43 localization without altering its ubiquitination. These data suggest that σ_1R^{E102Q} overexpression causes ATP depletion and proteasomal impairment, which in turn impairs ATP-dependent TDP-43 transport and its proteasomal degradation. These aberrations lead to extra-nuclear localization of TDP-43 and aggravate that activity under ER stress conditions.

4. Discussion

This study reports four major findings (Fig. 9): 1) overexpressed σ_1R^{E102Q} mutants aggregate in the cytoplasm and partly co-localize with the proteasome; 2) σ_1R^{E102Q} mutants gradually dissociate from the IP_3R3 and impair mitochondrial Ca^{2+} uptake, resulting in compromised ATP synthesis and proteasome activity, especially under ER stress conditions; 3) decreased ATP production and proteasome activity trigger aberrant localization of TDP-43 and likely promote autophagic cell death; and 4) ATP supplementation by MP rescues σ_1R^{E102Q}-induced proteasome dysfunction and TDP-43 mislocalization. Therefore, we propose that MP treatment could be an attractive candidate for ALS therapy in patients harboring the σ_1R^{E102Q} mutation.

Although ATP supplementation rescues the σ_1R^{E102Q}-induced proteasome dysfunction, its causative mechanism remains unclear. The reduced proteasome activity promoted by σ_1R^{E102Q} overexpression may be caused not only by decreased ATP levels but also by formation of σ_1R^{E102Q} aggregates, which are likely degradation-resistant. Dissociation of σ_1R^{E102Q} from the IP_3R3 and its cytosolic aggregation coordinately trigger mitochondrial ATP depletion and proteasomal impairment. Both events precede σ_1R^{E102Q}-induced autophagy and degradation of mitochondrial proteins. However, further studies are required to define mechanisms underlying dissociation of σ_1R^{E102Q} from ER. The glutamic acid at position 102 of human σ_1R is highly conserved in vertebrates and located in the second transmembrane domain [13]. In distribution studies conducted in mouse motor neuron-like cells (NSC34), the authors who characterized this mutation showed that it causes mutant protein to segregate in lower density fractions relative to wild-type protein following sucrose gradient fractionation and to form detergent-resistant complexes of 50 kDa. In our experiments, σ_1R^{E102Q} aggregation was only observed at 96 h post-transfection (Fig. 1A) but not at 48 h when σ_1R^{E102Q} is still bound to the IP_3R3. Taken together with the previous observations, our results suggest that dissociation of σ_1R^{E102Q} mutant from the ER triggers its cytoplasmic localization and disturbs the proteasomal function to clear accumulated TDP-43 from the cytoplasm. In contrast, ER stress induced by tunicamycin decreased endogenous σ_1R expression (Fig. 5). Similar σ_1R downregulation is observed in motor neurons of ALS patients and SOD1 transgenic mice [14], an effect likely due to abnormal aggregation of mutant protein and which accounts for ER stress. Interestingly, we recently discovered a novel C-terminally deleted form of σ_1R expressed in mouse brain consisting of amino acids 1 to 106 and lacking chaperone regions [18]. In contrast to σ_1R^{E102Q} mutant proteins, when overexpressed in Neuro2A cells a subset of those proteins aggregates in nuclei and promotes apoptosis [18]. Also, abnormal nuclear σ_1R accumulation in neurons is reported in several neurodegenerative diseases [36]. As a functioning chaperone protein, σ_1R might be aggregation-prone, an activity facilitated by mutation, expression of a transcriptional variant, or pathogenic stress.

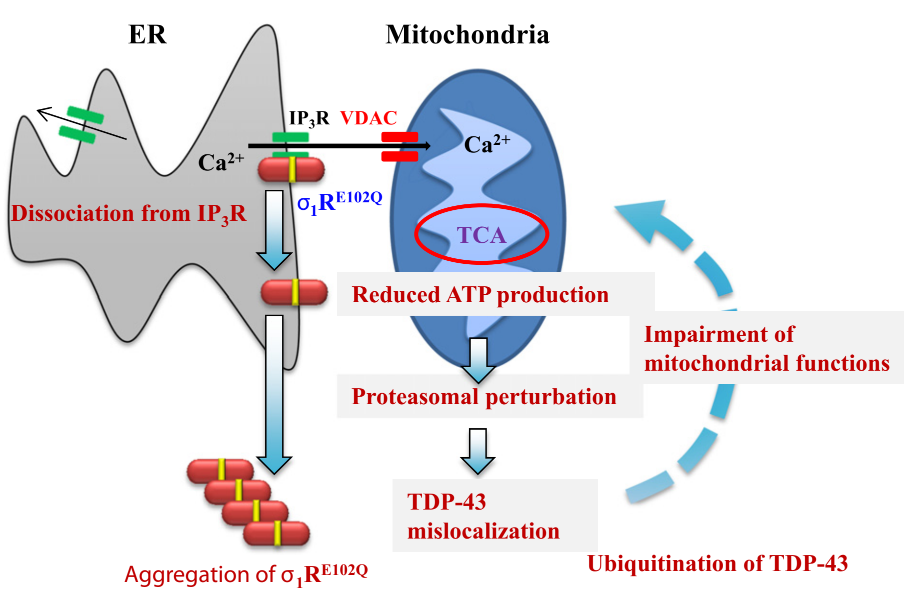

Fig. 9. Schematic representation of proposed function of σ_1R^{E102Q} in ALS induction. Under ER stress conditions, σ_1R^{E102Q} dissociates from the ER and aggregates in the cytoplasm. Loss of the σ_1R/IP_3R association impairs mitochondrial Ca^{2+} transport, reduces Ca^{2+}-dependent ATP production and disturbs proteasome activity followed by perturbation in autophagy, including mitochondrial degradation and TDP-43 mislocalization in the cytoplasm. Cytoplasmic TDP-43 may further impair mitochondrial and autophagosome function. IP_3R3: IP_3 receptor type 3, TDP-43: TAR DNA-binding protein.

We also found that expression of σ_1R^{E102Q} promoted mitochondrial damage, especially under conditions of tunicamycin-induced ER stress. σ_1R normally stabilizes the IP_3R3 in the ER membrane, enhancing Ca^{2+} transport from ER into mitochondria, activating the tricarboxylic acid (TCA) cycle, and increasing ATP production to promote cell survival [17,18]. Indeed, σ_1R overexpression in Neuro2A cells promotes mitochondrial elongation and IP_3R-dependent ATP production [17]. Conversely, treatment with Ru360, a selective inhibitor of the mitochondrial calcium uniporter (MCU), inhibited ATP production enhanced by σ_1R [18,37]. The MCU plays an important role in IP_3R-mediated Ca^{2+} transport to the mitochondrial matrix [38,39]. The lack of mitochondrial Ca^{2+} transport by IP_3R depletion inhibits pyruvate dehydrogenase and increases the AMP/ATP ratio, thereby aggravating autophagy *via* AMP kinase [40]. Activated AMP kinase phosphorylates the autophagy-initiating kinase ULK1, which is a homologue of yeast ATG1, at S317 and S777 and induces autophagy in HEK293 cells [41]. Taken together, impaired ATP production in those cells likely promotes mitochondrial degradation and aggravates ER stress-induced neuronal cell death.

SOD1 mutations are prevalent in ALS and promote mitochondrial dysfunction [5]. ALS patients also show proteasome dysfunction [42]. Dominant mutations in *TARDBP* are also reported in familial ALS [10]. Recently, Ayala et al. (2011) reported that treatment of cells with the ER stress inducer thapsigargin promotes accumulation/aggregation of phosphorylated cytoplasmic TDP-43 [43]. We found that, under ER stress conditions, autophagosome formation, as assessed by LC3-II production, significantly increased in cells expressing σ_1R^{E102Q} protein, and TDP-43 ubiquitination was also enhanced in either σ_1R knockdown or σ_1R^{E102Q}-overexpressing cells. Moreover, Tashiro et al. (2012) reported that mice with motor neuron-specific KO of the proteasome subunit Rpt3 show locomotor dysfunction, which is associated with TDP-43 mislocalization and accumulation in motor neurons [44]. On the other hand, mice harboring motor neuron-specific deletion of *autophagy related 7* (*Atg7*) gene, did not show these abnormalities [44]. Those authors conclude that impairment of the proteasome rather than autophagic function underlies ALS development caused by TDP-43 proteinopathy. Indeed, ATP supplementation with MP tended to inhibit autophagy and significantly prevented TDP-43 mislocalization. Interestingly, abnormal cytoplasmic localization of TDP-43 is associated with mitochondrial dysfunction under various conditions. For example, overexpression of TDP-43 or its C-terminal fragment promotes mitochondrial damage in neuronal NSC34 cells [45], and mitochondrial complex I activity is impaired by TDP-43 overexpression in the same cells [46]. SOD1 misfolding is observed after overexpression of TDP-43 in SH-SY5Y neuroblastoma cells [47]. Moreover, transgenic mice with brain-specific human TDP-43 expression show increased levels of mitochondrial fission protein such as Fis1 and decreased levels of the mitochondrial fusion protein mitofusin 1 in the brain [48]. Likewise, TDP-43 overexpression reduces mitochondrial length and neurite density in cultured motor neurons [49]. In addition, when overexpressed in Neuro2A cells, the protein encoded by *TARDBP* mutation seen in ALS patients is more stable than is the wild-type protein and inhibits autophagosome-dependent degradation of endogenous proteins [50]. Taken together, cytoplasmic mislocalization of TDP-43 is particularly relevant to σ_1R^{E102Q}-induced mitochondrial damage. However, further extensive studies are required to define molecular mechanisms underlying mitochondrial damage induced by cytoplasmic TDP-43.

Although previous reports suggest that p.G93A mutant SOD1 transgenic mice show cytoplasmic TDP-43 protein mislocalization [51], overexpression of another ALS-related protein, Ataxin-2, also induces TDP-43 protein mislocalization in HeLa cells [52]. These results are consistent with our observations of the ALS-related σ_1R mutation. However, Tan et al. [53] reported that familial ALS patients exhibiting p.A4T or p.D101Y mutations in SOD1 did not show TDP-43 protein mislocalization. Thus further studies are required to define temporal and regional changes in neuronal TDP-43 distribution in ALS patients. Regarding σ_1R activity in other neurodegenerative disorders, Hyrskyluoto et al. (2013) reported that σ_1R levels decrease in neuronal PC6.3 cells expressing an N-terminal huntingtin fragment with 120Q repeats [54]. They also showed that treatment with the σ_1R agonist PRE-084 restored σ_1R protein levels and promoted cell survival in mutated huntingtin-expressing cells through activation of the NF-κB pathway [54]. In this context, future studies should address MP-induced cell survival signaling.

ATP is critical for sequestration of cytoplasmic material in autophagosomes and in maintaining proton pump (vacuolar-type ATPase or V-ATPase) activity at the lysosomal membrane to produce acidification required for autophagic flux [55]. ATP is also essential for proteasomal degradation of ubiquitinated substrates [56]. Thus σ_1R^{E102Q}-induced ATP reduction likely causes proteasome dysfunction. In addition, nuclear protein import and export require the importin–Ran system [57]. ATP depletion inhibits importin β nuclear export [33, 34]. TDP-43 undergoes nuclear translocation *via* importin α/β proteins [58]. The present study strongly suggests that ATP supplementation antagonizes TDP-43 mislocalization and mitochondrial damage. We found that cellular ATP levels were upregulated by MP treatment and TDP-43 localization was normalized. MP is a cell-permeable form of pyruvate that acts as an alternative energy source to replace glucose and activate the TCA cycle [59]. Currently, the only approved treatment for ALS is the drug riluzole, which provides only modest benefits in terms of survival time without improving muscle strength or function [60,61]. Manccuso et al. report that the σ_1R agonist PRE-084 improves motor neuron function and survival in mouse ALS models harboring human *SOD1* mutations [62]. On the other hand, Luty et al. suggested that treatment of culture cells with the σ_1R antagonists AC915 and haloperidol, but not the agonist opipramol, decreases TDP-43 cytoplasmic levels [11]. Most recently, Prause et al. reported that PRE-084 rescues VAPB mutant aggregation in NSC34 cells [14]. Thus, the potential of therapeutics targeting σ_1R in ALS remains a possibility. Our study suggests a more attractive strategy using ATP supplementation as ALS therapy. Further study is required to define whether this approach could enhance the survival and quality of life of ALS patients.

Finally, several 3′ UTR variants and a missense mutation in *SIGMAR1* gene are reported in ALS and FTLD patients [11–13]. Interestingly, some 3′ UTR variants (c.672*51G>T and c.672*43G>T) but not the c.672*26C>T substitution co-segregate with hexanucleotide repeat expansions in *C9ORF72*, and those two variants are likely not responsible for the onset of ALS or FTLD [12,63]. Still, in humans *SIGMAR1* is located on chromosome 9p13.3 in close proximity to the *C9ORF72* locus at 9p21.2. The chromosome area 9p, which includes these regions, is reportedly an important locus for both ALS and FTLD [64–66]. However, the relationship between 3′ UTR *SIGMAR1* variants and hexanucleotide repeat expansions in *C9ORF72* remains unclear. Further studies are required to evaluate whether mutations in the former can cause ALS or FTLD. In contrast, a missense mutation in *SIGMAR1* completely segregated with the onset of ALS in the pedigree [13], strongly suggesting that it plays a significant role in the pathogenesis.

5. Conclusions

ATP depletion and proteasomal impairment promoted by σ_1R^{E102Q} overexpression caused extra-nuclear localization of TDP-43 and enhanced its ubiquitination only under ER stress conditions. We also discovered that pathogenic activities caused by σ_1R^{E102Q} could be rescued by ATP supplementation through treatment with MP, a substrate in the mitochondrial TCA cycle. This observation suggests a potential therapeutic strategy for σ_1R^{E102Q}-induced abnormal TDP-43 accumulation in ALS. The therapeutic potential of sodium pyruvate to treat mitochondrial diseases has been suggested [67] and is being assessed in clinical trials for patients with mitochondrial disease, including mitochondrial DNA depletion syndrome [68]. However, further preclinical studies are needed to compare pharmacodynamic and pharmacokinetic properties of methyl pyruvate and sodium pyruvate prior to testing in human therapy.

Acknowledgements

We thank Dr. Teruo Hayashi of the National Institute on Drug Abuse, Department of Health and Human Services, National Institutes of Health, for kindly providing antibodies against the N- and C-termini of σ_1R; and Dr. Atsushi Miyawaki at the Brain Science Institute, RIKEN, for kindly providing ratiometric-pericam-mt/pcDNA3.

This work was supported in part by Grants-in-Aid for Scientific Research from the Ministry of Education, Science, Sports and Culture of Japan (KAKENHI 24102505, 24659024 and 25293124 to K.F.), a Grant-in-Aid for Development of Systems and Technology for Advanced Measurement and Analysis from the Japan Science and Technology Agency (JST) (K.F.), a Grant-in-Aid for Scientific Research on Priority Areas (25110705 to N. S.) and a research fellowship from the Japan Society for the Promotion of Science (KAKENHI 244360 to H.T.).

References

[1] G. Manfredi, Z. Xu, Mitochondrial dysfunction and its role in motor neuron degeneration in ALS, Mitochondrion 5 (2) (2005) 77–87.
[2] P. Shi, Y. Wei, J. Zhang, J. Gal, H. Zhu, Mitochondrial dysfunction is a converging point of multiple pathological pathways in amyotrophic lateral sclerosis, J. Alzheimers Dis. 20 (Suppl. 2) (2010) S311–S312.
[3] L. Ferraiuolo, J. Kirby, A.J. Grierson, M. Sendtner, P.J. Shaw, Molecular pathways of motor neuron injury in amyotrophic lateral sclerosis, Nat. Rev. Neurol. 7 (11) (2011) 616–630.
[4] S. Millecamps, F. Salachas, C. Cazeneuve, P. Gordon, B. Bricka, A. Camuzat, L. Guillot-Noël, O. Russaouen, G. Bruneteau, P.F. Pradat, N. Le Forestier, N. Vandenberghe, V. Danel-Brunaud, N. Guy, C. Thauvin-Robinet, L. Lacomblez, P. Couratier, D. Hannequin, D. Seilhean, I. Le Ber, P. Corcia, W. Camu, A. Brice, G. Rouleau, E. LeGuern, V. Meininger, SOD1, ANG, VAPB, TARDBP, and FUS mutations in familial amyotrophic lateral sclerosis: genotype–phenotype correlations, J. Med. Genet. 47 (8) (2010) 554–560.
[5] A.E. Renton, A. Chiò, B.J. Traynor, State of play in amyotrophic lateral sclerosis genetics, Nat. Neurosci. 18 (1) (2014) 17–23.
[6] D.R. Rosen, T. Siddique, D. Patterson, D.A. Figlewicz, P. Sapp, A. Hentati, D. Donaldson, J. Goto, J.P. O'Regan, H.X. Deng, et al., Mutations in Cu/Zn superoxide dismutase gene are associated with familial amyotrophic lateral sclerosis, Nature 362 (6415) (1993) 59–62.
[7] A.M. Blokhuis, E.J. Groen, M. Koppers, L.H. van den Berg, R.J. Pasterkamp, Protein aggregation in amyotrophic lateral sclerosis, Acta Neuropathol. 125 (6) (2013) 777–794.
[8] J.P. Taylor, J. Hardy, K.H. Fischbeck, Toxic proteins in neurodegenerative disease, Science 296 (5575) (2002) 1991–1995.
[9] C. Lagier-Tourenne, M. Polymenidou, D.W. Cleveland, TDP-43 and FUS/TLS: emerging roles in RNA processing and degeneration, Hum. Mol. Genet. 19 (R1) (2010) R46–R64.
[10] M. Neumann, D.M. Sampathu, L.K. Kwong, A.C. Truax, M.C. Micsenyi, T.T. Chou, J. Bruce, T. Schuck, M. Grossman, C.M. Clark, L.F. McCluskey, B.L. Miller, E. Masliah, I. R. Mackenzie, H. Feldman, W. Feiden, H.A. Kretzschmar, J.Q. Trojanowski, V.M. Lee, Ubiquitinated TDP-43 in frontotemporal lobar degeneration and amyotrophic lateral sclerosis, Science 314 (5796) (2006) 130–133.
[11] A.A. Luty, J.B. Kwok, C. Dobson-Stone, C.T. Loy, K.G. Coupland, H. Karlström, T. Sobow, J. Tchorzewska, A. Maruszak, M. Barcikowska, P.K. Panegyres, C. Zekanowski, W.S. Brooks, K.L. Williams, I.P. Blair, K.A. Mather, P.S. Sachdev, G.M. Halliday, P.R. Schofield, Sigma nonopioid intracellular receptor 1 mutations cause frontotemporal lobar degeneration-motor neuron disease, Ann. Neurol. 68 (5) (2010) 639–649.
[12] V.V. Belzil, H. Daoud, W. Camu, M.J. Strong, P.A. Dion, G.A. Rouleau, Genetic analysis of SIGMAR1 as a cause of ALS with dementia, Eur. J. Hum. Genet. 21 (2) (2013) 237–239.
[13] A. Al-Saif, F. Al-Mohanna, S. Bohlega, A mutation in sigma-1 receptor causes juvenile amyotrophic lateral sclerosis, Ann. Neurol. 70 (6) (2011) 913–919.
[14] J. Prause, A. Goswami, I. Katona, A. Roos, M. Schnizler, E. Bushuven, A. Dreier, S. Buchkremer, S. Johann, C. Beyer, M. Deschauer, D. Troost, J. Weis, Altered localization, abnormal modification and loss of function of Sigma receptor-1 in amyotrophic lateral sclerosis, Hum. Mol. Genet. 22 (8) (2013) 1581–1600.
[15] W.R. Martin, C.G. Eades, J.A. Thompson, R.E. Huppler, P.E. Gilbert, The effects of morphine- and nalorphine-like drugs in the nondependent and morphine-dependent chronic spinal dog, J. Pharmacol. Exp. Ther. 197 (3) (1976) 517–532.
[16] S.W. Tam, L. Cook, Sigma opiates and certain antipsychotic drugs mutually inhibit (+)-[3H]SKF 10,047 and [3H]haloperidol binding in guinea pig brain membranes, Proc. Natl. Acad. Sci. U. S. A. 81 (17) (1984) 5618–5621.
[17] T. Hayashi, T.P. Su, Sigma-1 receptor chaperones at the ER–mitochondrion interface regulate Ca^{2+} signaling and cell survival, Cell 131 (2007) 596–610.
[18] N. Shioda, K. Ishikawa, H. Tagashira, T. Ishizuka, H. Yawo, K. Fukunaga, Expression of a truncated form of the endoplasmic reticulum chaperone protein, sigma-1 receptor, promotes mitochondrial energy depletion and apoptosis, J. Biol. Chem. 287 (28) (2012) 23318–23331.
[19] T.A. Mavlyutov, M.L. Epstein, K.A. Andersen, L. Ziskind-Conhaim, A.E. Ruoho, The sigma-1 receptor is enriched in postsynaptic sites of C-terminals in mouse motoneurons. An anatomical and behavioral study, Neuroscience 167 (2) (2010) 247–255.
[20] H. Tagashira, M.S. Bhuiyan, N. Shioda, H. Hasegawa, H. Kanai, K. Fukunaga, Sigma-1 receptor stimulation with fluvoxamine ameliorates transverse aortic constriction-induced myocardial hypertrophy and dysfunction in mice, Am. J. Physiol. Heart Circ. Physiol. 299 (5) (2010) H1535–H1545.
[21] N. Shioda, Y. Yamamoto, M. Watanabe, B. Binas, Y. Owada, K. Fukunaga, Heart-type fatty acid binding protein regulates dopamine D2 receptor function in mouse brain, J. Neurosci. 30 (8) (2010) 3146–3155.
[22] W. Pendergrass, N. Wolf, M. Poot, Efficacy of MitoTracker Green and CMXrosamine to measure changes in mitochondrial membrane potentials in living cells and tissues, Cytometry A 61 (2) (2004) 162–169.
[23] H. Tagashira, M.S. Bhuiyan, N. Shioda, K. Fukunaga, Distinct cardioprotective effects of 17β-estradiol and dehydroepiandrosterone on pressure-overload-induced hypertrophy in ovariectomized female rats, Menopause 18 (12) (2011) 1317–1326.
[24] T. Nagai, A. Sawano, E.S. Park, A. Miyawaki, Circularly permuted green fluorescent proteins engineered to sense Ca^{2+}, Proc. Natl. Acad. Sci. U. S. A. 98 (6) (2001) 3197–3202.
[25] S. Thomas, S. Kotamraju, J. Zielonka, D.R. Harder, B. Kalyanaraman, Hydrogen peroxide induces nitric oxide and proteosome activity in endothelial cells: a bell-shaped signaling response, Free Radic. Biol. Med. 42 (7) (2007) 1049–1061.
[26] G. Csordás, C. Renken, P. Várnai, L. Walter, D. Weaver, K.F. Buttle, T. Balla, C.A. Mannella, G. Hajnóczky, Structural and functional features and significance of the physical linkage between ER and mitochondria, J. Cell Biol. 174 (7) (2006) 915–921.
[27] S.H. Lecker, A.L. Goldberg, W.E. Mitch, Protein degradation by the ubiquitin–proteasome pathway in normal and disease states, J. Am. Soc. Nephrol. 17 (7) (2006) 1807–1819.
[28] V. Menéndez-Benito, L.G. Verhoef, M.G. Masucci, N.P. Dantuma, Endoplasmic reticulum stress compromises the ubiquitin–proteasome system, Hum. Mol. Genet. 14 (19) (2005) 2787–2799.
[29] M. Urushitani, J. Kurisu, K. Tsukita, R. Takahashi, Proteasomal inhibition by misfolded mutant superoxide dismutase 1 induces selective motor neuron death in familial lateral sclerosis, J. Neurochem. 83 (5) (2002) 1030–1042.
[30] J.M. Gump, A. Thorburn, Autophagy and apoptosis: what is the connection? Trends Cell Biol. 21 (7) (2011) 387–392.
[31] G. Szabadkai, K. Bianchi, P. Várnai, D. De Stefani, M.R. Wieckowski, D. Cavagna, A.I. Nagy, T. Balla, R. Rizzuto, Chaperone-mediated coupling of endoplasmic reticulum and mitochondrial Ca^{2+} channels, J. Cell Biol. 175 (6) (2006) 901–911.
[32] O.M. de Brito, L. Scorrano, Mitofusin 2 tethers endoplasmic reticulum to mitochondria, Nature 456 (7222) (2008) 605–610.
[33] S. Kose, N. Imamoto, Y. Yoneda, Distinct energy requirement for nuclear import and export of importin beta in living cells, FEBS Lett. 463 (3) (1999) 327–330.
[34] S. Kose, M. Furuta, M. Koike, Y. Yoneda, N. Imamoto, The 70-kD heat shock cognate protein (hsc70) facilitates the nuclear export of the import receptors, J. Cell Biol. 171 (1) (2005) 19–25.
[35] N. Benaroudj, P. Zwickl, E. Seemüller, W. Baumeister, A.L. Goldberg, ATP hydrolysis by the proteasome regulatory complex PAN serves multiple functions in protein degradation, Mol. Cell 11 (1) (2003) 69–78.
[36] Y. Miki, F. Mori, T. Kon, K. Tanji, Y. Toyoshima, M. Yoshida, H. Sasaki, A. Kakita, H. Takahashi, K. Wakabayashi, Accumulation of the sigma-1 receptor is common to neuronal nuclear inclusions in various neurodegenerative diseases, Neuropathology 34 (2) (2014) 148–158.
[37] H. Tagashira, C. Zhang, Y.M. Lu, H. Hasegawa, H. Kanai, K. Fukunaga, Stimulation of σ_1-receptor restores abnormal mitochondrial Ca^{2+} mobilization and ATP production following cardiac hypertrophy, Biochim. Biophys. Acta 1830 (4) (2013) 3082–3094.
[38] J.M. Baughman, F. Perocchi, H.S. Girgis, M. Plovanich, C.A. Belcher-Timme, Y. Sancak, X.R. Bao, L. Strittmatter, O. Goldberger, R.L. Bogorad, V. Koteliansky, V.K. Mootha, Integrative genomics identifies MCU as an essential component of the mitochondrial calcium uniporter, Nature 476 (7360) (2011) 341–345.
[39] D. De Stefani, A. Raffaello, E. Teardo, I. Szabò, R. Rizzuto, A forty-kilodalton protein of the inner membrane is the mitochondrial calcium uniporter, Nature 476 (7360) (2011) 336–340.
[40] C. Cárdenas, R.A. Miller, I. Smith, T. Bui, J. Molgó, M. Müller, H. Vais, K.H. Cheung, J. Yang, I. Parker, C.B. Thompson, M.J. Birnbaum, K.R. Hallows, J.K. Foskett, Essential regulation of cell bioenergetics by constitutive InsP3 receptor Ca^{2+} transfer to mitochondria, Cell 142 (2) (2010) 270–283.
[41] J. Kim, M. Kundu, B. Viollet, K.L. Guan, AMPK and mTOR regulate autophagy through direct phosphorylation of Ulk1, Nat. Cell Biol. 13 (2) (2011) 132–141.
[42] E.V. Ilieva, V. Ayala, M. Jové, E. Dalfó, D. Cacabelos, M. Povedano, M.J. Bellmunt, I. Ferrer, R. Pamplona, M. Portero-Otín, Oxidative and endoplasmic reticulum stress interplay in sporadic amyotrophic lateral sclerosis, Brain 130 (Pt 12) (2007) 3111–3123.
[43] V. Ayala, A.B. Granado-Serrano, D. Cacabelos, A. Naudí, E.V. Ilieva, J. Boada, V. Caraballo-Miralles, J. Lladó, I. Ferrer, R. Pamplona, M. Portero-Otin, Cell stress induces TDP-43 pathological changes associated with ERK1/2 dysfunction: implications in ALS, Acta Neuropathol. 122 (3) (2011) 259–270.
[44] Y. Tashiro, M. Urushitani, H. Inoue, M. Koike, Y. Uchiyama, M. Komatsu, K. Tanaka, M. Yamazaki, M. Abe, H. Misawa, K. Sakimura, H. Ito, R. Takahashi, Motor neuron-

specific disruption of proteasomes, but not autophagy, replicates amyotrophic lateral sclerosis, J. Biol. Chem. 287 (51) (2012) 42984–42994.
[45] K. Hong, Y. Li, W. Duan, Y. Guo, H. Jiang, W. Li, C. Li, Full-length TDP-43 and its C-terminal fragments activate mitophagy in NSC34 cell line, Neurosci. Lett. 530 (2) (2012) 144–149.
[46] J. Lu, W. Duan, Y. Guo, H. Jiang, Z. Li, J. Huang, K. Hong, C. Li, Mitochondrial dysfunction in human TDP-43 transfected NSC34 cell lines and the protective effect of dimethoxy curcumin, Brain Res. Bull. 89 (5–6) (2012) 185–190.
[47] E. Pokrishevsky, L.I. Grad, M. Yousefi, J. Wang, I.R. Mackenzie, N.R. Cashman, Aberrant localization of FUS and TDP43 is associated with misfolding of SOD1 in amyotrophic lateral sclerosis, PLoS One 7 (4) (2012) e35050.
[48] Y.F. Xu, T.F. Gendron, Y.J. Zhang, W.L. Lin, S. D'Alton, H. Sheng, M.C. Casey, J. Tong, J. Knight, X. Yu, R. Rademakers, K. Boylan, M. Hutton, E. McGowan, D.W. Dickson, J. Lewis, L. Petrucelli, Wild-type human TDP-43 expression causes TDP-43 phosphorylation, mitochondrial aggregation, motor deficits, and early mortality in transgenic mice, J. Neurosci. 30 (32) (2010) 10851–10859.
[49] W. Wang, L. Li, W.L. Lin, D.W. Dickson, L. Petrucelli, T. Zhang, X. Wang, The ALS disease-associated mutant TDP-43 impairs mitochondrial dynamics and function in motor neurons, Hum. Mol. Genet. 22 (23) (2013) 4706–4719.
[50] S. Watanabe, K. Kaneko, K. Yamanaka, Accelerated disease onset with stabilized familial amyotrophic lateral sclerosis (ALS)-linked mutant TDP-43 proteins, J. Biol. Chem. 288 (5) (2013) 3641–3654.
[51] X. Shan, D. Vocadlo, C. Krieger, Mislocalization of TDP-43 in the G93A mutant SOD1 transgenic mouse model of ALS, Neurosci. Lett. 458 (2) (2009) 70–74.
[52] Y. Nihei, D. Ito, N. Suzuki, Roles of ataxin-2 in pathological cascades mediated by TAR DNA-binding protein 43 (TDP-43) and Fused in Sarcoma (FUS), J. Biol. Chem. 287 (49) (2012) 41310–41323.
[53] C.F. Tan, H. Eguchi, A. Tagawa, O. Onodera, T. Iwasaki, A. Tsujino, M. Nishizawa, A. Kakita, H. Takahashi, TDP-43 immunoreactivity in neuronal inclusions in familial amyotrophic lateral sclerosis with or without SOD1 gene mutation, Acta Neuropathol. 113 (2007) 535–542.
[54] A. Hyrskyluoto, I. Pulli, K. Törnqvist, T.H. Ho, L. Korhonen, D. Lindholm, Sigma-1 receptor agonist PRE084 is protective against mutant huntingtin-induced cell degeneration: involvement of calpastatin and the NF-κB pathway, Cell Death Dis. 4 (2013) e646.
[55] P.J. Plomp, E.J. Wolvetang, A.K. Groen, A.J. Meijer, P.B. Gordon, P.O. Seglen, Energy dependence of autophagic protein degradation in isolated rat hepatocytes, Eur. J. Biochem. 164 (1) (1987) 197–203.
[56] S.E. Babbitt, A. Kiss, A.E. Deffenbaugh, Y.H. Chang, E. Bailly, H. Erdjument-Bromage, P. Tempst, T. Buranda, L.A. Sklar, J. Baumler, E. Gogol, D. Skowyra, ATP hydrolysis-dependent disassembly of the 26S proteasome is part of the catalytic cycle, Cell 121 (4) (2005) 553–565.
[57] D. Dormann, C. Haass, TDP-43 and FUS: a nuclear affair, Trends Neurosci. 34 (2011) 339–348.
[58] A.L. Nishimura, V. Zupunski, C. Troakes, C. Kathe, P. Fratta, M. Howell, J.M. Gallo, T. Hortobágyi, C.E. Shaw, B. Rogelj, Nuclear import impairment causes cytoplasmic trans-activation response DNA-binding protein accumulation and is associated with frontotemporal lobar degeneration, Brain 133 (Pt 6) (2010) 1763–1771.
[59] S.H. Jo, C. Yang, Q. Miao, M. Marzec, M.A. Wasik, P. Lu, Y.L. Wang, Peroxisome proliferator-activated receptor gamma promotes lymphocyte survival through its actions on cellular metabolic activities, J. Immunol. 177 (6) (2006) 3737–3745.
[60] A. Stewart, J. Sandercock, S. Bryan, C. Hyde, P.M. Barton, A. Fry-Smith, A. Burls, The clinical effectiveness and cost-effectiveness of riluzole for motor neurone disease: a rapid and systematic review, Health Technol. Assess. 5 (2) (2001) 1–97.
[61] A. Messori, S. Trippoli, P. Becagli, G. Zaccara, Cost effectiveness of riluzole in amyotrophic lateral sclerosis. Italian Cooperative Group for the Study of Meta-Analysis and the Osservatorio SIFO sui Farmaci, Pharmacoeconomics 16 (2) (2006) 153–163.
[62] R. Mancuso, S. Oliván, A. Rando, C. Casas, R. Osta, X. Navarro, Sigma-1R agonist improves motor function and motoneuron survival in ALS mice, Neurotherapeutics 9 (4) (2012) 814–826.
[63] C. Dobson-Stone, M. Hallupp, C.T. Loy, E.M. Thompson, E. Haan, C.M. Sue, P.K. Panegyres, C. Razquin, M. Seijo-Martínez, R. Rene, J. Gascon, J. Campdelacreu, B. Schmoll, A.E. Volk, W.S. Brooks, P.R. Schofield, P. Pastor, J.B. Kwok, C9ORF72 repeat expansion in Australian and Spanish frontotemporal dementia patients, PLoS One 8 (2) (2013) e56899.
[64] C. Vance, A. Al-Chalabi, D. Ruddy, B.N. Smith, X. Hu, J. Sreedharan, T. Siddique, H.J. Schelhaas, B. Kusters, D. Troost, F. Baas, V. de Jong, C.E. Shaw, Familial amyotrophic lateral sclerosis with frontotemporal dementia is linked to a locus on chromosome 9p13.2-21.3, Brain 129 (Pt 4) (2006) 868–876.
[65] A.A. Luty, J.B. Kwok, E.M. Thompson, P. Blumbergs, W.S. Brooks, C.T. Loy, C. Dobson-Stone, P.K. Panegyres, J. Hecker, G.A. Nicholson, G.M. Halliday, P.R. Schofield, Pedigree with frontotemporal lobar degeneration — motor neuron disease and Tar DNA binding protein-43 positive neuropathology: genetic linkage to chromosome 9, BMC Neurol. 29 (8) (2008) 32.
[66] H. Laaksovirta, T. Peuralinna, J.C. Schymick, S.W. Scholz, S.L. Lai, L. Myllykangas, R. Sulkava, L. Jansson, D.G. Hernandez, J.R. Gibbs, M.A. Nalls, D. Heckerman, P.J. Tienari, B.J. Traynor, Chromosome 9p21 in amyotrophic lateral sclerosis in Finland: a genome-wide association study, Lancet Neurol. 9 (10) (2010) 978–985.
[67] M. Tanaka, Y. Nishigaki, N. Fuku, T. Ibi, K. Sahashi, Y. Koga, Therapeutic potential of pyruvate therapy for mitochondrial diseases, Mitochondrion 7 (6) (2007) 399–401.
[68] K. Saito, N. Kimura, N. Oda, H. Shimomura, T. Kumada, T. Miyajima, K. Murayama, M. Tanaka, T. Fujii, Pyruvate therapy for mitochondrial DNA depletion syndrome, Biochim. Biophys. Acta 1820 (5) (2012) 632–636.